**A**

**THESIS REPORT**

***On***

# Design and Analysis of Hypoid and Helical Gears for Modular Tandem Axle

***Submitted in partial fulfillment of the requirement***

***for the award of degree of***

**Master of Engineering**

***in***

**Thermal Engineering**


*Submitted by*

**Manu Dev Sharma**

**Roll No.: 801583014**

*Under the joint supervisions of*

**Mr. Sumeet Sharma**
**Associate Professor**
**Department of Mechanical Engineering**
**Thapar University, Patiala-147004, India.**

**Dr. D Gangacharyulu**
**Professor**
**Department of Chemical Engineering**
**Thapar University, Patiala-147004, India.**

**DEPARTMENT OF MECHANICAL ENGINEERING**

**THAPAR UNIVERSITY**

**PATIALA-147004, INDIA**


**July-2017**

# CERTIFICATE

I hereby declare that work done in this thesis entitled **"Design and Analysis of Hypoid and Helical Gears for Modular Tandem Axle Concept"** submitted towards partial fulfillment of requirement for award of **Master of Engineering degree** in **Thermal Engineering** in **Mechanical Engineering Department** of **Thapar University, Patiala,** is an authentic record of my work carried out under the supervision and guidance of **Mr. Sumeet Sharma, Associate Professor, Mechanical Engineering Department, Thapar University** and co-guidance of **Dr. D Gangacharyulu, Professor, Chemical Engineering Department, Thapar University** along with **Mr. Kunal Kamal, Senior Manager, Product Design and Development, VE Commercial Vehicles Ltd., Pithampur** during January 2017 to May 2017.

The matter embodied in this thesis has not been submitted in part or full to any other university or institute for the award of any degree.

Manu Dev.

Dated:

Manu Dev Sharma

This is to certify that above declaration made by the student is correct to the best of my knowledge and belief.

Kunal Kamal

**Mr. Kunal Kamal**
*Senior Manager*
*Product Design and Development*
*VE Commercial Vehicles Ltd.*
*Pithampur, Dist. Dhar-454775*
*Madhya Pradesh, India.*

Sumeet Sharma

**Mr. Sumeet Sharma**
*Associate Professor*
*Mechanical Engineering Department*
*Thapar University, Patiala, India*

D. Gangacharyulu

**Dr. D Gangacharyulu** 16/8/17
*Professor*
*Chemical Engineering Department*
*Thapar University, Patiala, India*

*Dedicated to*

*my parents*

# Acknowledgement

Words often fall short to reveal one's deepest regards. A work like this can never be accompanied by the efforts of a single person and I would be obliged to express my profound gratitude and respect to all the people who helped me throughout the duration of this work.

Firstly I would like to express my sincere gratitude to Mr. Sumeet Sharma for his invaluable guidance and encouragement. I am also very much indebted to my superior Mr. Kunal Kamal, Senior Manager, VECV for his unreserved guidance, suggestions and inspiration in the nurturing work. I am thankful to Mr. Sachin Agarwal, Senior Vice President, for providing me the opportunity to be a part of this project. My sincere thanks also goes to Dr. D. Gangacharyulu whose valuable inputs came to me as rescue at difficult times.

I would also like to thank the whole rear axle team of VECV for their valuable and consistent support whenever I needed it.

Finally, I am grateful to my family and friends without their encouragement, patience and moral support, it would not have been possible for me to complete this work.

Manu Dev.

Manu Dev Sharma

# Abstract

Rear axle is the last member of the power train which finally transfers the engine's power to the driving wheels. In heavy duty trucks, we often use more than one driving axle which brings us to the need for tandem axle. A tandem axle divides the incoming power into two parts, each one going to different driving axle. Using tandem axle in a vehicle also improves road stability at highway speeds and usually has better suspensions. At VECV, a wide range of heavy duty vehicles employ tandem axle which makes it quite beneficial to develop a modular design which helps in achieving a simpler design. To achieve this modular design, critical components inside a tandem axle such as hypoid gear set, helical gear pair and differential gears are designed taking consideration of the specifications of the whole range of vehicles and then grouping them into similar groups. The design procedure followed for all components is taken from various publications studied during our literature survey. Most prominent reasons for the failure of automotive gears are bending stresses and contact stresses. Therefore, each gear set designed is rated for both pitting resistance (contact stresses) and bending strength with the help of standards developed by organizations such as AGMA. Hypoid gear geometry is one of the most complicated geometry in all of the gear types. A geometry design calculation sheet has also been developed to generate complete design specifications sheet which includes a program for an iterative process.

*Key words*: Modular design; Hypoid gears; Bevel gears; Helical gears; Bending strength; Pitting resistance.

# Table of Contents


**CERTIFICATE** .......... i

**Acknowledgement** .......... iii

**Abstract** .......... iv

**Table of Contents** .......... v

**List of Figures** .......... vii

**List of Tables** .......... viii

**Nomenclature** .......... ix

**1. Introduction** .......... 1

1.1 Introduction .......... 1

1.2 Methodology .......... 2

1.3 Understanding of Rear Axle Design .......... 2

1.4 Understanding Rear Axle Manufacturing .......... 5

1.4.1 Critical Assembly Processes .......... 6

1.5 Forward tandem axle carrier .......... 8

1.6 Outline of the thesis work .......... 11

**2. Literature Review** .......... 12

2.1 Introduction .......... 12

2.2 Literature survey on design and analysis of hypoid or helical gears .......... 12

2.3 Literature survey on gear materials .......... 15

2.4 Literature survey on modularity .......... 16

2.5 Objectives of present work .......... 17

**3. Design Procedure and Calculations** .......... 18

3.1 Introduction .......... 18

3.2 Design of hypoid gear .......... 18

3.2.1 Selection of drive gear type .......... 18

3.2.2 Selection of drive gear size .......... 20

3.2.3 Rating of Hypoid gears ........ 26

3.2.4 Hypoid Gear Specifications ........ 32

3.2.5 Hypoid geometry ........ 38

3.2.6 Significance of Depth factor, mean addendum factor and clearance factor ........ 40

3.2.7 Analysis of forces [ANSI-AGMA 2005-D03] ........ 42

3.3 Helical Gears ........ 45

3.3.1 Design Methodology ........ 46

3.3.2 Force Analysis ........ 48

3.3.3 Lewis and Buckingham equation analysis for dynamic loads ........ 49

3.3.4 Rating of helical gears ........ 53

**4. Results ........ 58**

**5. Conclusion ........ 60**

**References ........ 61**

**Appendix A ........ 64**

**Appendix B ........ 69**

# List of Figures


| | | | |
|---|---|---|---|
| Fig. | 1.1 | Representation of a forward tandem axle carrier | 2 |
| Fig. | 1.2 | Cut section view of rear axle | 3 |
| Fig. | 1.3 | Exploded view of rear axle | 4 |
| Fig. | 1.4 | Flow process of rear axle manufacturing at VECV | 5 |
| Fig. | 1.5 | Flow process of hub sub assembly at rear axle manufacturing line at VECV | 6 |
| Fig. | 1.6 | Backlash | 7 |
| Fig. | 1.7 | Ideal contact pattern | 8 |
| Fig. | 1.8 | Back face run out testing | 8 |
| Fig. | 1.9 | Exploded view of forward axle carrier assembly | 9 |
| Fig. | 2.1 | Spin loss measurement methodology | 14 |
| Fig. | 2.2 | Axle losses categories | 15 |
| Fig. | 2.3 | Engineering stress–strain diagrams for 20MnCr5 steel at room and elevated temperatures | 16 |
| Fig. | 3.1 | Hypoid gear nomenclature | 19 |
| Fig. | 3.2 | Charts for selecting approximate gear size for hypoid gears with 22.5° avg. | 23 |
| Fig. | 3.3 | Factor of safety diagram for bending group 1 | 28 |
| Fig. | 3.4 | Factor of safety diagram for durability group 1 | 28 |
| Fig. | 3.5 | Factor of safety diagram for bending group 2 | 29 |
| Fig. | 3.6 | Factor of safety diagram for durability group 2 | 29 |
| Fig. | 3.7 | Factor of safety diagram for bending group3 | 30 |
| Fig. | 3.8 | Factor of safety diagram for durability group 3 | 30 |
| Fig. | 3.9 | Hypoid geometry | 38 |
| Fig. | 3.10 | Bevel gear nomenclature - axial plane | 39 |
| Fig. | 3.11 | Bevel gear nomenclature -- mean section (A-A in figure 11) | 40 |
| Fig. | 3.12 | Resultant gear tooth forces | 42 |
| Fig. | 3.13 | Resultant gear tooth forces | 43 |
| Fig. | 3.14 | Tooth forces on a right hand helical gear | 48 |
| Fig. | 3.15 | Geometry factors for pitting resistance and bending strength for helical gears with 25 deg. helix angle and 20 deg. pressure angle | 55 |

# List of Tables


| | | | |
|---|---|---|---|
| Table | 1.1 | Bill of material for tandem axle carrier assembly | 10 |
| Table | 3.1 | Comparison between hypoid and spiral bevel gear | 18 |
| Table | 3.2 | Gradeability | 20 |
| Table | 3.3 | Road rolling resistance factors | 21 |
| Table | 3.4 | Specifications of the vehicle range for which tandem axle is to be designed | 24 |
| Table | 3.5 | Preliminary diameters for all the vehicles | 25 |
| Table | 3.6 | Suggested minimum numbers of pinion teeth (spiral and hypoid) | 32 |
| Table | 3.7 | Calculation sheet for hypoid specifications | 32 |
| Table | 3.8 | Relationship between load face and hand of the pinion | 43 |
| Table | 3.9 | Maximum pinion torque values | 45 |
| Table | 3.10 | Standard tooth proportion for helical gears | 47 |
| Table | 3.11 | Factors of safety for helical gear | 57 |
| Table | 4.1 | Results (Modular design) | 58 |

# Nomenclature

$T_{PFG}$ =Performance torque

$T_{PMG}$ =Maximum prime mover torque

$T_{WSG}$ = Maximum wheel slip torque

$W_C$ =Gross vehicle weight or gross combination weight

$r_R$ =Tire rolling radius

$N_D$ =Number of driving axles

$G_H$ =Highway grade factor

$G_R$ =Road rolling resistance factor

$K_O$ =Overload factor for shock loads resulting from snapping the clutch

$T_E$ =Minimum net engine output torque

$m_T$ =Transmission ratio in lowest gear

$m_c$ =Automatic transmission convertor ratio

$m_G$ =Bevel or hypoid drive gear ratio used in the axle

$N_D$ =Number of driving axle

$T_{WSG}$ = Maximum wheel slip torque

$W_D$ = Loaded weight on driving axle = $W_L \cdot f_d$

$W_L$ = Loaded weight of vehicle :GCW or GVW

$f_d$ = Drive axle weight distribution factor

$f_s$ = Coefficient of friction between tires and road

$M_G$ = Bevel or hypoid gear ratio

$N_D$ = Number of driving axles

$M_A$ = Overall axle ratio including bevel or hypoid drive gear, wheel reduction gear or two speed axle reduction gear

$s_{tG}$ ,$s_{tP}$ = Calculated tensile bending stresses at the root of the tooth for pinion and gear respectively

$s_c$ = Calculated contact stress at the point on tooth where its value will be maximum

$C_p$ = Elastic coefficient of gear and pinion material combination

$T_P$, $T_G$ = Transmitted torques of pinion and gear respectively

$T_{Pmx}$ = Maximum transmitted pinion torque

$K_o$, $C_o$ = Overload factors for strength and durability respectively

$K_V$, $C_V$ = Dynamic factors for strength and durability respectively

$P_d$ = Gear transverse diametral pitch at outer end of tooth

$F_P$, $F_G$ = Face widths of pinion and gear respectively

D = Gear outer pitch diameter

$n_N$ = Numbers of teeth in pinion and gear respectively

$K_s$, $C_s$ = Size factors for strength and durability respectively

$K_m$, $C_m$ = Load distribution factors for strength and durability respectively

$C_f$ = Surface condition factor for durability

$J_P$, $J_G$ = Geometry factors for strength of pinion and gear respectively

$J_P'$ = Modified pinion geometry factor for strength

I = Geometry factor for durability

$s_{wt}$, $s_{wc}$ = Working tensile bending stress and working contact stress respectively

$s_{at}$, $s_{wc}$ = Allowable tensile bending stress and allowable contact stress respectively

$K_L$, $C_L$ = Life factors for strength and durability respectively

$C_H$ = Hardness ratio factor for durability

$K_T$, $C_T$ = Temperature factors for strength and durability respectively

$K_R$, $C_R$ = Factors of safety for strength and durability respectively

## Greek Symbols

$\sigma_c$ = Surface stress or contact stress

$\sigma_b$ = Bending Stress (Tensile)

$\phi_n$ = Normal pressure angle

$\beta$ = Helix angle

## Acronyms

GCW = Gross Combination Weight

GVW = Gross Vehicle Weight

FEA = Finite Element Analysis

HD = Heavy Duty

LMD = Light and Medium Duty

# Chapter 1

# Introduction

## 1.1 Introduction

Rear axle is the last aggregate of a power train. In commercial vehicles, real axle is the driving axle. The engine turns a propeller shaft which transmits rotational force to a drive axle at the rear of the vehicle. The pinion of the hypoid gear set or spiral bevel gear set drives the crown wheel and subsequently transferring power to differential arrangement. One half-axle or half-shaft links the differential with the left rear wheel, a second half-shaft does the same with the right rear wheel; thus the two half-axles and the differential create the rear axle.

The aim of this project is to create a modular design of rear tandem axle for the complete range of heavy duty trucks in VECV. For power transmission, a tandem axle has various types of gears namely, hypoid, straight bevel and helical gears which can be observed in figure 1.1. By modular design, it is simply meant that for the entire range of our product line, minimum numbers of designs are to be developed so as to reduce the operational cost and introduce simplicity to the system. Modularity also helps in reducing lead time for future projects (Langlois, 2002).

A tandem axle truck is equipped with two drive axles. Utilizing eight tires and wheels on the drive axles, this type of truck is able to support a tremendous amount of weight as well as provide improved traction despite poor road conditions. While the engine sends power to the lead axle, the trailing axle receives its power via a short drive shaft extending from the rear of the lead axle housing.

A tandem axle is type of an axle in which power coming from the engine via propeller shaft is divided into two parts with the help of an inter-axle differential. One part of this power is transferred to differential gears through a helical gear set from where it is given to the wheels. While the other part of this power goes to an output shaft which goes into further axle to drive another two wheels which can be seen in below figure 1.1.

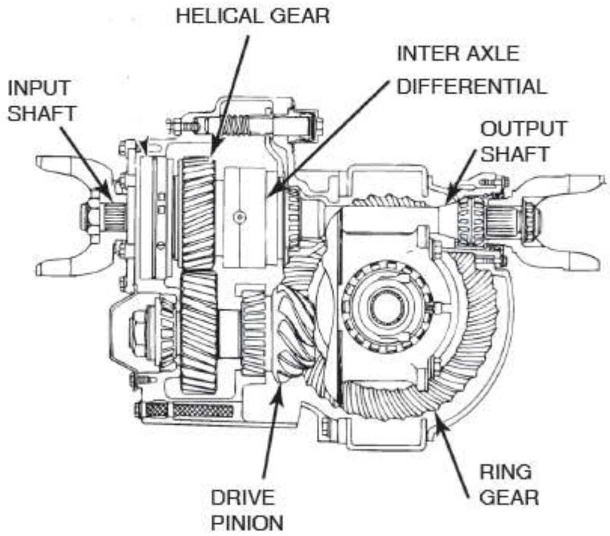


Figure 1.1: Representation of a forward tandem axle carrier (Dana Corporation, 2005)

## 1.2 Methodology

Following methodology has been adopted step by step to achieve our desired aim:

1. Understanding of rear axle design.
2. Understanding of rear axle manufacturing at VECV.
    - Process flow, critical assembly process
3. Understanding of basics of tandem axle and its various components.
    - Basic working, BOM of forward carrier assembly
4. Literature Survey
5. VECV tandem axle requirement.
6. Calculation for tandem axle components:
    - Hypoid gear,
    - Helical gear.
7. Selecting a modular design meeting requirement of all the vehicles.

## 1.3 Understanding of Rear Axle Design

The rear axle assembly comprises of the differential assembly, the rear drive axles, and axle housing. Rear axle assemblies are exposed to a major portion of the loads from the engine and road. Therefore, they have to be ruggedly constructed and should not ever fail. The most common rear end mischances are axle bearing failures. A typical rear axle assembly is shown in figure 1.2 (Duffy, 2000).

In a rear axle assembly, engine power enters the drive pinion gear from the drive shaft assembly and differential pinion flange. The pinion then transfers the power to the crown wheel or the ring gear. This is either a spiral bevel gear set or a hypoid gear set. Thus, the interaction of the crown wheel and the pinion turns the power flow at a 90° angle. At this stage, reduction also occurs which reduces the speed but increases the torque instead.

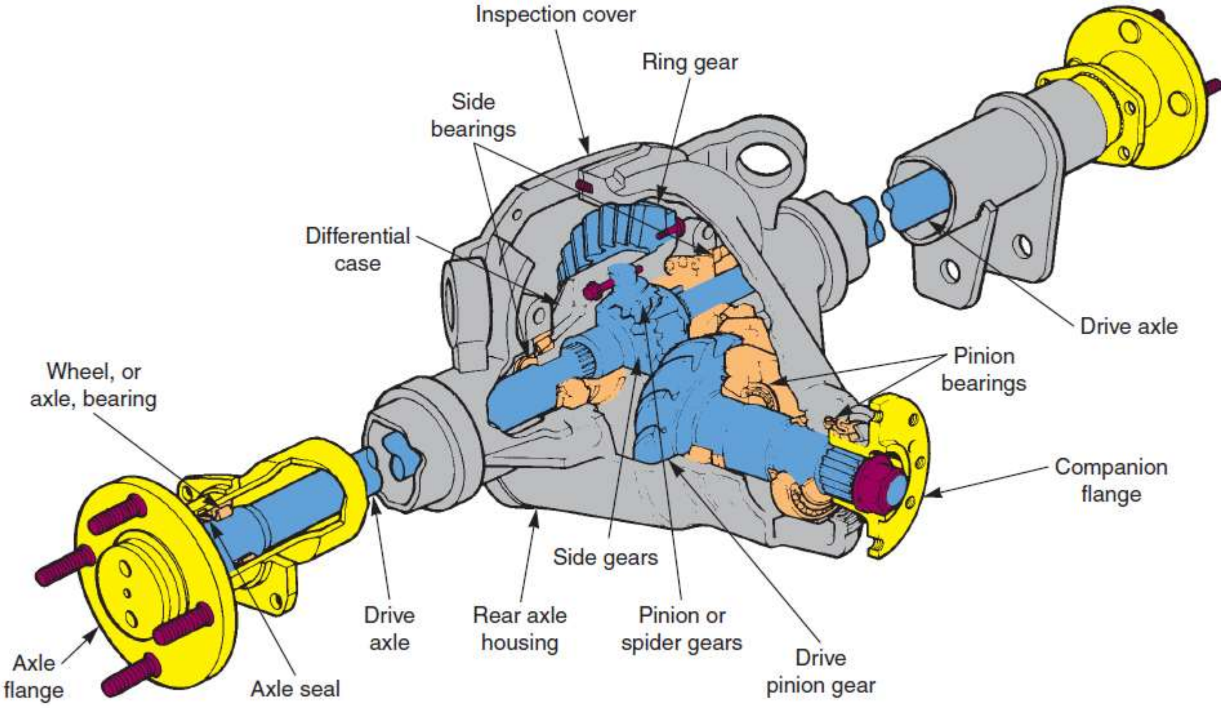


Figure 1.2: Cut section view of rear axle (Duffy, 2000)

Power from the crown wheel now transfers via the differential casing, spider bevel gears, and side bevel gears to the axle shafts. These shafts transfer power from the differential assembly to the wheels.

The bearings and rear axle housing are crucial parts of the rear axle assembly. They are designed to hold and align the whole assembly and axles. Bearings and axle housing are so ruggedly designed that they should not fail under any circumstances.

Seals and gaskets in the rear axle assembly insure the working of the rear axle assembly. Seals are used at the differential pinion yoke/flange and at the outer drive axles. Gaskets are used between different housing parts to provide a tight seal so that the lubricant should not leak or any contaminants from outside can come in.

The figure 1.3 is an exploded view of a common type of rear axle assembly. Notice the relationship of the internal parts to the housing and to each other. Note that the rear axle housing and drive axle designs will be different when the vehicle has independent rear suspension.

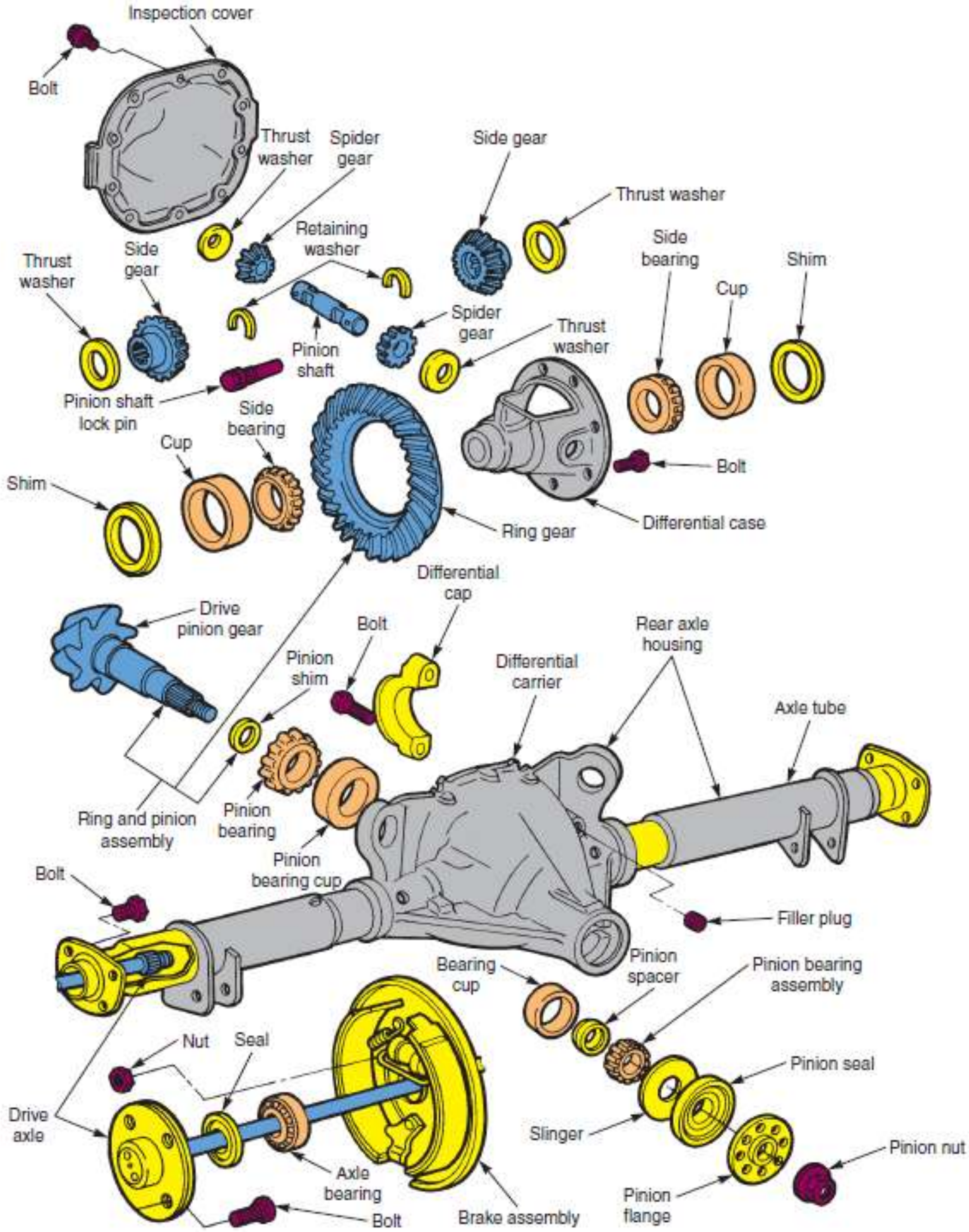


Figure 1.3: Exploded view of rear axle (Duffy, 2000)

## 1.4 Understanding Rear Axle Manufacturing

**Flow process of the Rear Axle Manufacturing Line at VECV**

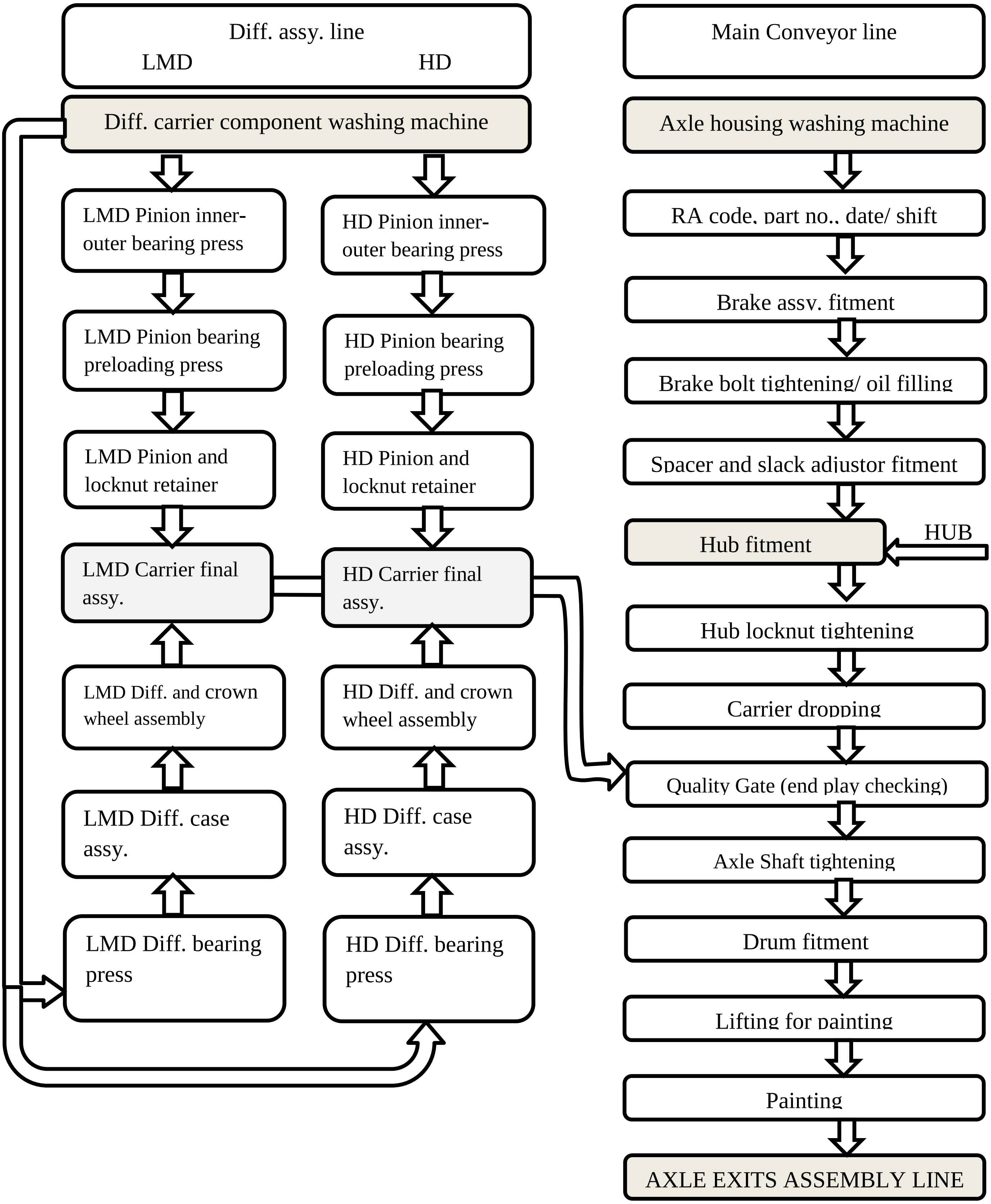


Figure 1.4: Flow process of rear axle manufacturing at VECV

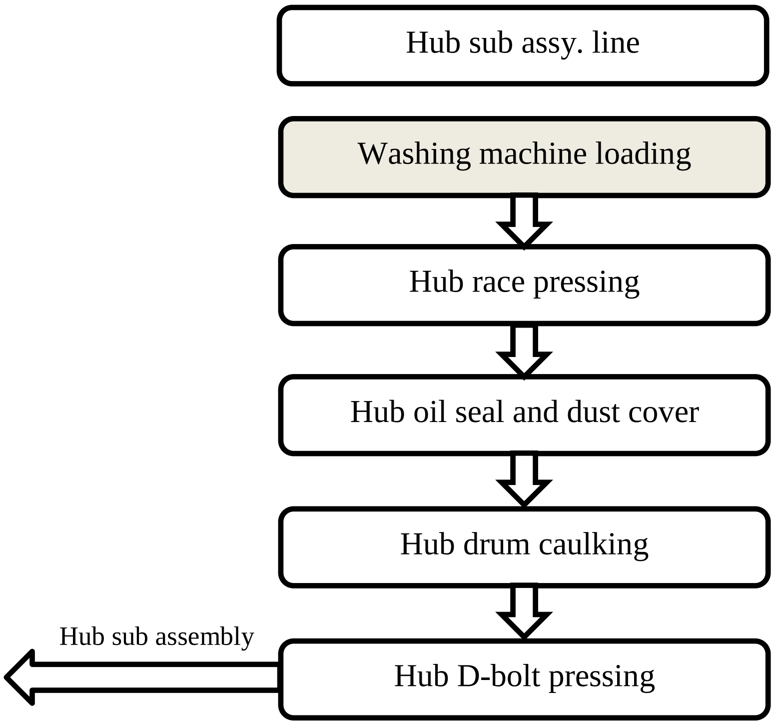


Figure 1.5: Flow process of hub sub assembly at rear axle manufacturing line at VECV

In rear axle assembly line, we have two separate lines to assemble the differential carrier, one for HD vehicles and one for LMD vehicles, one line for hub sub assembly and one main final line. There are few critical processes in the assembly line discussed below.

### 1.4.1 Critical Assembly Processes

- **Collar Selection:** The rear axle pinion bearing is pressed onto the drive pinion gear shaft at the gear end. The front pinion bearing is often a slip fit on the smaller end of the shaft. The outer races, or bearing cups, of both bearings are pressed into the rear axle housing. A collar is used make some preload on the bearing. Sometime a collapsible spacer is also used for the preloading. The collar is made such that it is slightly compressed when the pinion gear is mounted in the rear axle housing. The spacer retains a mild pressure between both of the rear and front bearings, making it possible to precisely adjust the bearing preload. Collar is selected by pre loading it with a hydraulic press and then checking if it moves within a specific torque using a torque wrench.
- **Shim Selection:** The location of the hypoid pinion relative to the crown wheel must be set exactly. Or else there will be noise and gears will wear out. The position of the pinion gear in the axle housing must be carefully adjusted as the contact at exact right tooth depth is

essential. To make this adjustment to the ring and drive pinion clearance, a pinion shim is installed in the housing, behind the rear bearing cup. The depth of the pinion in the axle housing is determined by the thickness of the shim. The shim is installed at the line only and after that it must be checked for proper thickness every time the drive pinion gear is removed. A shim of specific thickness is inserted to eliminate the errors in the dimensions of differential carrier, error of pinion and error of bearing retainer. Based on these parameters, thickness of the shim is selected.

| (0.3*A) + B – C | | | |
|---|---|---|---|
| Error in Dimension of differential carrier (A) | Error in pinion (B) | Error of bearing retainer (C) | Thickness of the Shim |
| | | | |

- **Backlash crown wheel – pinion**: Backlash can be defined as "the maximum distance or angle through which any part of a mechanical system may be moved in one direction without applying appreciable force or motion to the next part in mechanical sequence". Backlash between crown wheel and pinion in every carrier assembly is checked to be within specified range.

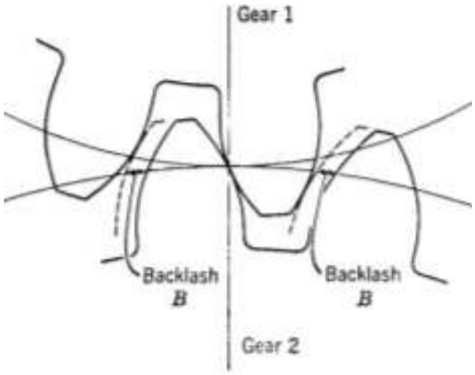


Figure 1.6: Backlash

- **Contact Pattern:** Contact pattern between pinion and ring gear is tested to be optimum. The procedure of checking contact pattern is as follow: Apply tooth contact compound to the ring gear in two different places. Carefully apply moderate pressure to the outside ring gear. Rotate the pinion to turn the ring gear specified revolutions on the drive side and then in the opposite direction for the coast side. The following are typical ring gear patterns. Check with the manufacturer’s manual for specifications or any special procedures.

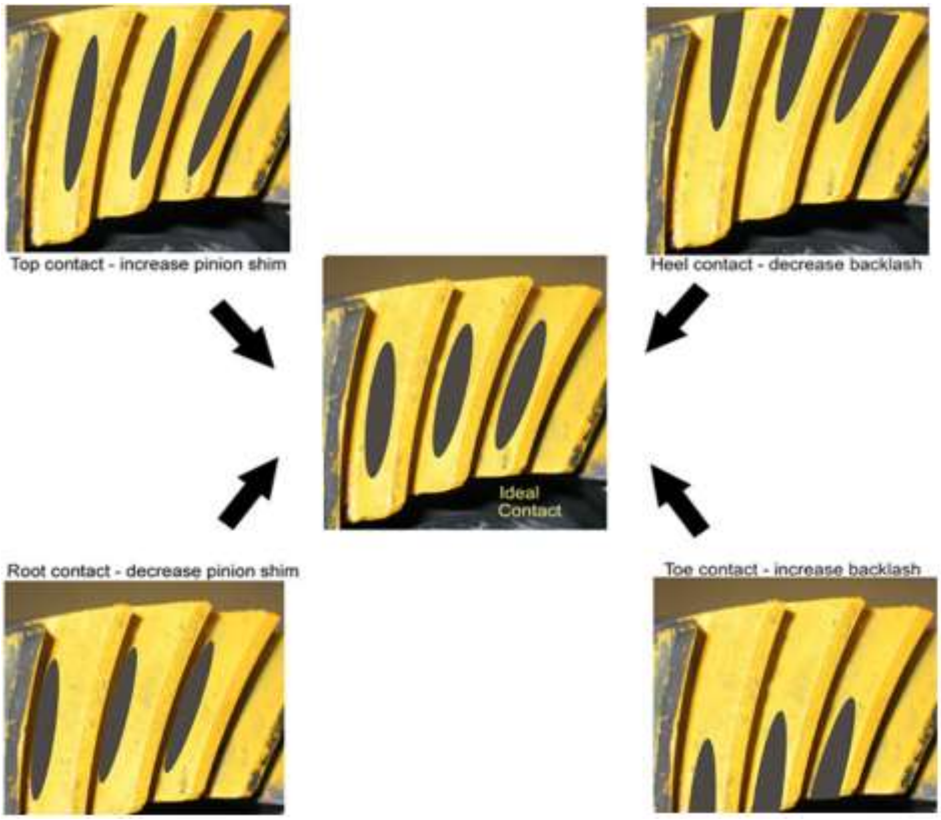


Figure 1.7: Ideal contact pattern

- **Back face run out**: Run out is an inaccuracy of rotating mechanical systems. Back face runout of the ring gear is tested with the help of a linear dial gauge.

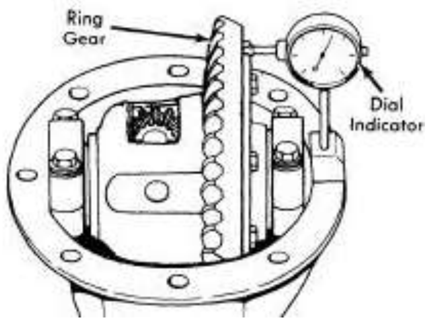


Figure 1.8: Back face runout testing

- **End play of hub**: End play of the hub is again checked with the help of a dial gauge (<0.1mm).

## 1.5 Forward tandem axle carrier

For understand complete construction of forward tandem axle assembly, we can study an exploded view of forward axle carrier assembly of Dana ® Spicer ® Tandem Drive Axles in figure 1.9 (Dana Corporation, 2007) along with its Bill of Materials.

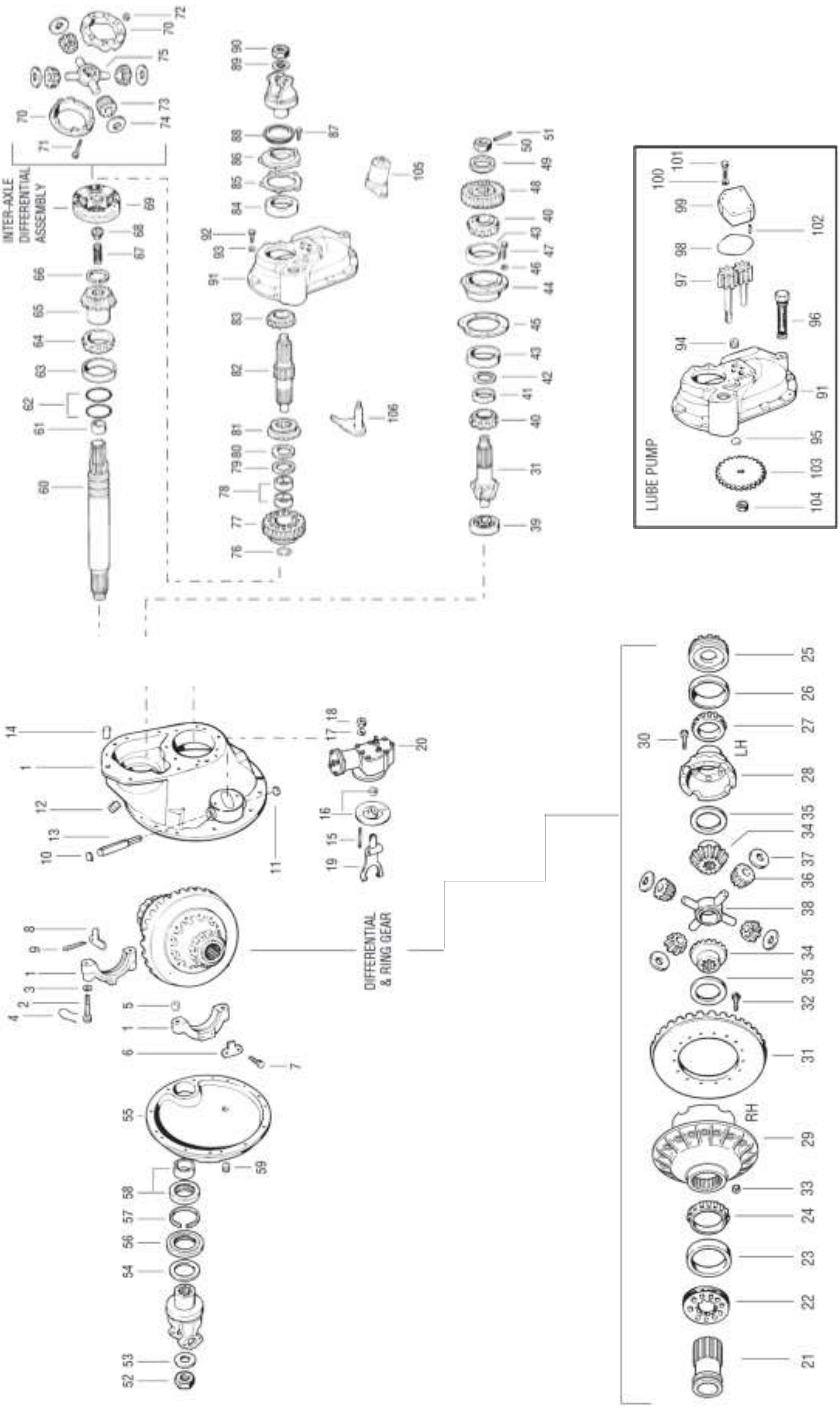


Figure 1.9: Exploded view of forward axle carrier assembly

Table 1.1: Bill of material for tandem axle carrier assembly

| BILL OF MATERIALS | | | | | |
|---|---|---|---|---|---|
| PART NO. | DESCRIPTION | QTY. | PART NO. | DESCRIPTION | QTY. |
| 1 | Differential carrier & 2 bearing caps | 1 | 55 | Axle housing cover | 1 |
| 2 | Bearing capscrew | 4 | 56 | Output shaft oil seal | 1 |
| 3 | Flat washer | 4 | 57 | Bearing snap ring | 1 |
| 4 | Lockwire | 4 | 58 | Output shaft bearing | 1 |
| 5 | Dowel bushing | 4 | 59 | Filler plug | 1 |
| 6 | Bearing cap adjuster lock (RH) | 1 | 60 | Output shaft | 1 |
| 7 | Capscrew | 4 | 61 | Output shaft bushing | 1 |
| 8 | Bearing cap adjuster lock (LH) | 1 | 62 | Output shaft O-ring | 2 |
| 9 | Cotter pin (LH) | 1 | 63 | Output shaft bearing cup | 1 |
| 10 | Expansion plug (upper) | 1 | 64 | Output shaft bearing cone | 1 |
| 11 | Expansion plug (lower) | 1 | 65 | Output shaft side gear | 1 |
| 12 | Filler plug | 1 | 66 | Side gear snap ring | 1 |
| 13 | Shift fork shaft | 1 | 67 | Output shaft compression spring | 1 |
| 14 | Carrier cover dowel pin | 2 | 68 | Output shaft thrust bearing | 1 |
| 15 | Shift unit mounting stud | 1 | 69 | Inter-axle differential assembly | 1 |
| 16 | Shift fork seal & spring assembly | 1 | 76 | Helical side gear snap ring | 1 |
| 17 | Flat washer | 1 | 77 | Helical side gear | 1 |
| 18 | Stud nut | 1 | 78 | Helical side gear bushing | 2 |
| 19 | Shift fork & roller assembly | 1 | 79 | Helical side gear thrust washer | 1 |
| 20 | Shift unit assembly | 1 | 80 | Helical side gear “D” washer | 1 |
| 21 | Sliding clutch | 1 | 81 | Lockout sliding clutch | 1 |
| 22 | Differential bearing adjuster (RH) | 1 | 82 | Input shaft | 1 |
| 23 | Differential bearing cup (RH) | 1 | 83 | Input shaft bearing cone | 1 |
| 24 | Differential bearing cone (RH) | 1 | 84 | Input shaft bearing cup | 1 |
| 25 | Differential bearing adjuster (LH) | 1 | 85 | Input cover shim | 1 |
| 26 | Differential bearing cup (LH) | 1 | 86 | Input bearing cover | 1 |
| 27 | Differential bearing cone (LH) | 1 | 87 | Bearing cover capscrew | 5 |
| 28 | Differential case (plain half) | 1 | 88 | Input shaft oil seal | 1 |
| 29 | Differential case (flanged half) | 1 | 89 | Input shaft nut washer | 1 |
| 30 | Differential case capscrew | 8 | 90 | Input shaft nut | 1 |
| 31 | Ring gear & drive pinion | 1 set | 91 | PDU carrier cover | 1 |
| 32 | Bolt | 18 | 92 | Carrier cover capscrew | 11 |
| 33 | Nut | 18 | 93 | Lock washer | 11 |
| 34 | Differential side gear | 2 | 94 | Pipe plug | 1 |
| 35 | Side gear thrust washer | 2 | 95 | Expansion plug | 1 |
| 36 | Side pinion | 4 | 96 | Magnetic filter screen | 1 |
| 37 | Side pinion thrust washer | 4 | 97 | Pump gear & shaft assembly | 2 |
| 38 | Spider | 1 | 98 | Cover O-ring | 1 |
| 39 | Pinion pilot bearing | 1 | 99 | Lube pump cover | 1 |
| 40 | Pinion bearing cone | 1 | 100 | Lock washer | 6 |

| | | | | | |
|---|---|---|---|---|---|
| 41 | Pinion bearing spacer washer | 1 | 101 | Cover capscrew | 6 |
| 42 | Pinion bearing spacer | 1 | 102 | Cover dowel pin | 1 |
| 43 | Pinion bearing cup | 1 | 103 | Pump drive gear | 1 |
| 44 | Pinion bearing cage | 1 | 104 | Drive gear locknut | 1 |
| 45 | Pinion bearing cage shim | 1 | 105 | Air-operated lockout assembly | 1 |
| 46 | Lock washer | 6 | 106 | Shift fork & push rod assembly | 1 |
| 47 | Bearing cage capscrew | 6 | INTER-AXLE DIFFERENTIAL ASSEMBLY | | |
| 48 | Pinion helical gear | 1 | 70 | Inter-axle differential case half | 2 |
| 49 | Outer pinion support bearing (1 pc.) | 1 | 71 | Case bolt | 8 |
| 50 | Pinion shaft end nut | 1 | 72 | Case nut | 8 |
| 51 | Pinion nut spring pin | 1 | 73 | Side pinion | 4 |
| 52 | Output shaft nut | 1 | 74 | Side pinion thrust washer | 4 |
| 53 | Output shaft washer | 1 | 75 | Spider | 1 |
| 54 | Rear bearing retaining washer | 1 | | | |

## 1.6 Outline of the thesis work

This thesis work has been carried out in various steps to reach our goal of designing hypoid and helical gears for tandem axle carrier. Chapter wise division of the work done is discussed below:

Chapter 1 consists of the introduction of the concept, basics of rear axle which includes the basic construction and its working. Current rear axle assembly line at Eicher Trucks and Buses plant and critical processes involved are also briefed.

Chapter 2 includes the literature survey various research papers and other sources to help us understand about the current procedures, standards being used in the industry to design automotive gears. The current trend in adaptation of modularity in operations and technology has also been surveyed in few papers.

Chapter 3 includes the whole design methodology and procedure adopted to design both hypoid and helical gears for given inputs. To analyse the gears, their ratings for both bending and pitting are calculated using AGMA standards.

Chapter 4 contains results part for the designs. A design summary sheet is prepared in which gear specifications for all the vehicles are tabulated.

Chapter 5 presents conclusions obtained from the research work conducted during thesis work. In addition to this, this chapter also deals with future scopes of the thesis.

# Chapter 2
# Literature Review

## 2.1 Introduction

This chapter discusses the literature review done for the completion of the thesis and the objectives of the thesis. Literature review was done in 3 areas: (i) Design and analysis of hypoid or helical gears, (ii) Gear materials and (iii) Modularity.

## 2.2 Literature survey on design and analysis of hypoid or helical gears

**Gawande et al. (2013)** performed mechanical design of crown wheel and pinion in differential gearbox of Mechanical Front Wheel Drive (MFWD) Axle of a tractor (TAFE MF 455). Details of modelling and assembly were explained. The crown wheel and pinion were designed using slip torque as application of load in case of tractor is usually in the peak range. After the design of the crown wheel and pinion, the same is drafted in PRO-E and analysed in ANSYS where it was seen that equivalent stress on tooth was coming out to be approximately 682 N/mm2 whereas maximum allowed stress was 698.667 N/mm2.

**Barot and Vora (2014)** explained how to design a single stage hypoid gear to be used in rear axle of trucks. Hypoid gears are being used in the rear axles of all leading companies due to advantage over spiral bevel gear. Major advantages of using hypoid gear are better fuel consumption and lower noise. The design procedure followed is based on ANSI-AGMA 2005-D034 (Design Manual for Bevel Gears). This procedure designs a gear set based on working torque by selecting appropriate pinion pitch diameter. Rest of formulae used are from ANSI-AGMA 2005-D03 which gives us the whole design sheet.

**Brown (2009)** gave out a detailed approach to spiral bevel gear design and its analysis for use in a medium class helicopter. SAE 9310 steel was chosen as gear material with proper carburisation and case hardening processes. Both bending analysis and fatigue analysis were done to make sure that design gear pair is safe due to both bending and pitting respectively. For pitting analysis, the author investigated the Hertz stresses. Also, it was shown that for the purpose of the application, the gears were designed for unlimited life.

**Venkatesh et al. (2010)** published his project that involved designing, modelling and manufacturing of helical gears in marine applications. The design conditions consisted of rotations at very high speed inducing large stresses and deflections in the helical gears. All the parameters i.e. gear specifications are calculated theoretically using design data by PSG College of Technology, Coimbatore. Then analysis of design gear is done by equations derived by Lewis and Buckingham for dynamic loads and as well as by FEA using ANSYS.

**Sekercioglu and Kovan (2007)** investigated cause of failure of spiral bevel gear used in differential of trucks. All the possible causes of the failure were investigated either experimentally or analytically. Visual inspection, metallurgical tests, chemical analysis and hardness tests were performed on various specimens prepared from the damaged spiral bevel gears. The failure was observed to be due to pitting occurrence. It was found in the investigation that there was no consistency in the microstructure and hardness of the gear materials as chemical composition varied. It was concluded from this studied that hardness of gear outer surface should be between 58-60 HRC in order to obtain maximum pitting resistance. Calculated contact stresses also revealed that gear was exposed to overloading. Due to this high tooth- contact pressure, lubrication also suffered as oil film thickness may not be enough.

**Lim and Cheng (1999)** used a generic 3-D coupled rotational-translational model for vibrations for simulation of the dynamic responses of typical geared rotor designs with hypoid gears. The line of action and operative gear mesh point are presumed fixed and overlap with the theoretical pitch point and the surface normal vector, respectively. The model is proposed to be used for predicting the response of an automobile drivetrain including hypoid gears and to evaluate the effects of hypoid offset on vibrations (free and forced). It is concluded by the author that although the hypoid offset has minimal effect on the predicted values of natural frequencies, it creates a substantial frequency-dependent effect on the frequency response functions of the dynamic mesh force and bearing reaction loads.

**Malek and Solanki (2015)** reviewed various papers on helical gear design based on contact stresses and bending stresses. Bending stress basically measures the strength of a gear while contact stresses determine the durability. To minimise failure of the gears, these two stresses are the main considerations. These both stresses can be calculated using either analytical methods or Finite Elements Analysis tools such as ANSYS. Bending stresses are calculated by using modified Lewis equation while for contact stresses, AGMA contact stress formulae were used.

**Hwang et al. (2013)** analysed to different methods for calculating contact stresses. For his study he used both spur gears and helical gears. It was found that stresses were more severe in case of lowest point of single tooth contact (LPSTC) approach than that calculated with the help of AGMA equations. These values were calculated using finite element analysis tools.

Jyothirmai et al. (2014) also made similar attempt to co relate the analytics results of bending and contact stress based on AGMA with the results from a develop FEA model in ANSYS. For these investigations he used both helical and herringbone gears. Similar researched it also done by **Venkatesh and Muthy (2014).**

**Kakavas et al. (2016)** measured and quantified the effect of viscosity on the efficiency of a hypoid gear drive in a vehicle. For this purpose he designed a test rig.

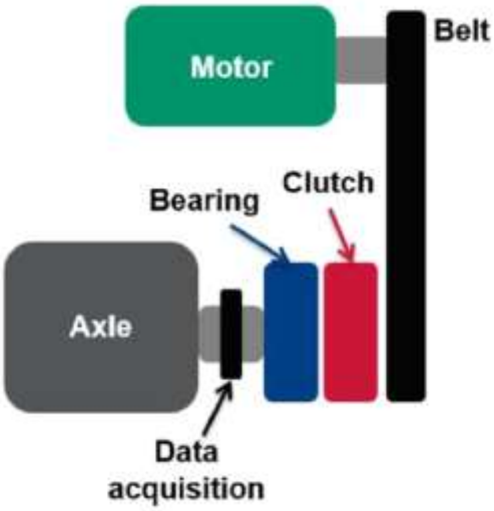


Figure 2.1: Spin loss measurement methodology

According to his studies, assumptions and simplifications used by other researchers lead to the wrong values the velocity of the point of contact in hypoid gears. Lubricant viscosity was found to be the main culprit in the loss of the efficiency. Experimental measurements were also co related with the generated simulations for number of scenarios and satisfactory results were observed.

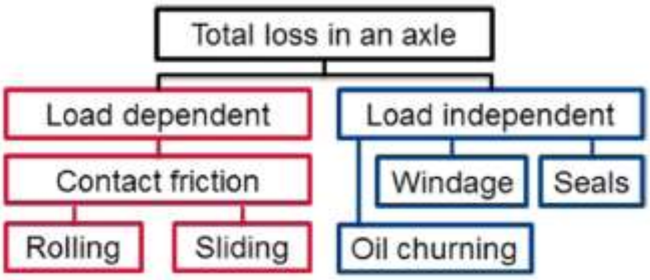


Figure 2.2: Axle losses categories

## 2.3 Literature survey on gear materials

**Bagewadi et al. (2014)** redesigned the spiral bevel gear for Mahindra Bolero pickup vehicle to increase its torque. This was achieved by reducing the no of teeth on pinion from 11 to 10 while keeping rest of the design same to fit new gear set in the same housing. Existing pinion material was also changed from SAE 4130 steel to SAE 9310 steel which helped in increasing margin of safety to 0.68 from existing 0.57 even though number of teeth on the pinion was reduced by 1.

**Brnic et al. (2014)** investigated the mechanical properties such as yield strength, ultimate tensile strength, Charpy test, creep test and total frcture strain, etc. on 20MnCr5 steel and similar steels. 20MnCr5 steel is being used for manufacturing of automobile gears these days. Comparison of properties of 20MnCr5 and other steels with similar properties is done by the author. Experiments were conducted at room temperature and higher temperatures. Tensile tests such as ultimate tensile strength along with other 0.2 offset yield strength were used to formulate stress- strain curves. Fracture toughness was assessed using using Charpy impact energy test.

**Brnic and Brcic (2015)** tried to compare two types of steel namely, 20MnCr5 Steel and X10CrAlSi25 Steel. It was found that both type of steels had similar mechanical properties such as yield strength, UTS, modulus of elasticity. It was also observed the their creep resistance was quite similar to each other.

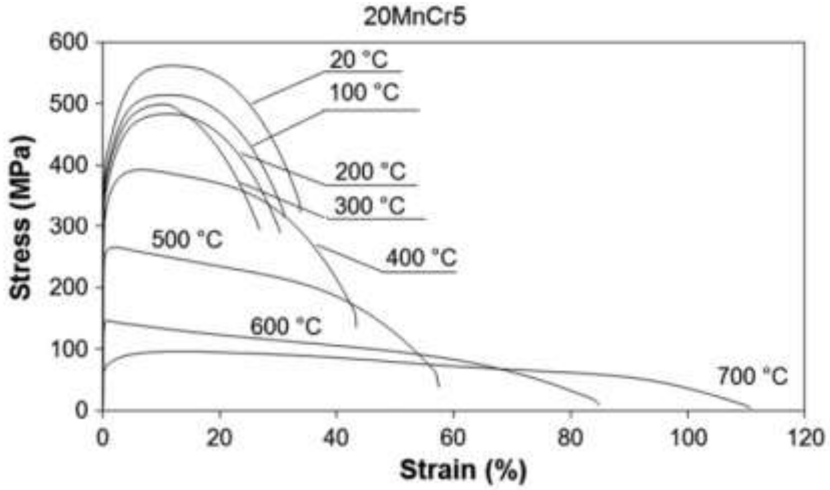


Figure 2.3: Engineering stress–strain diagrams for 20MnCr5 steel at room and elevated temperatures.

**Gligorijević et al. (2008)** pointed out the key issues for selection of materials and manufacturing processes in design of industrial products. The major design considerations that were given by the author includes bending fatigue lifetime index, bending fatigue limit index, surface fatigue lifetime index, surface fatigue limit index, machinability index and wear resistance of tooth flack index. Understanding of functional requirement is also necessary for material selection procedure. Other factors that affect the material selection are mechanical, chemical and physical properties, formability, castability, machinability, weldability, material impact on environment, product cost, availability, market trends, material cost, recycling etc.

## 2.4 Literature survey on modularity

**Gamba (2009)** researched on modularity in her doctoral thesis. It was found that over the last decade, many contributions had been done in field of modularity and extensive study was done on that. The study was performed taking in care of 'six modular operators' proposed by **Baldwin and Clark (2000).**

**Hölttä-Otto (2005)** also worked on modular product platform in which sets of common modules were shared in a product family to generate cost savings and establish a multiple product platform in very less time. A multi criteria scorecard was introduced to evaluate the modular platform to help organisation focus on strategy and its competition.

**Salvador et al. (2005)** suggested that an organisation can cope up with the losses on operations because of product variety by pursuing the path of modularity. The research focuses on which parameter should the modularity be designed and embedded into the product line. It is based on a qualitative research design that includes a multiple case study to investigate six product lines all belonging to the European companies. The modularity is suggested to be design on parameters such as type of modularity, level of modularity and component requiring modularity.

## 2.5 Objectives of present work

The work of this thesis has been carried out in VE Commercial Vehicles Ltd., Pithampur in Product Design and Development department. In their range of heavy duty trucks, tandem axles are used which were supplied by a third party vendor. Therefore, for in house development of tandem axle it was decide to go for a modular design which will reduce the operations cost. Hypoid gear pair is one of the most crucial part of the axle as it is an important link in the powertrain. Similarly, in tandem axle, a helical gear pair is also used. Keeping this in mind, the objectives of the work carried out in this thesis are:

- Creating preliminary dimensions for the complete range of the vehicles and then going for the modularity of the design. After finalizing the design, rating of the gair pair is to be calculated.
- Developing the calculation sheet for complete hypoid design dimensions including the iterative process.
- Designing and analysis of helical gear pair.

# Chapter 3
# Design Procedure and Calculations

## 3.1 Introduction
This chapter includes the methodology followed to obtain a complete modular design of both hypoid and helical gears.

## 3.2 Design of hypoid gear

### 3.2.1 Selection of drive gear type
The first consideration in gear design is the type of gear to be employed. Most heavy-duty drive axles employ either spiral bevel or hypoid gears in the drive-train. Hypoid gears are increasing in use in recent times due to their advantages over spiral bevel gears.

Table 3.1: Comparison between hypoid and spiral bevel gear

| CHARACTERISTICS | HYPOID | SPIRAL BEVEL |
|---|---|---|
| Quietness | Quieter | Quiet |
| Strength | As much as 30% higher loads depending on offset – also better strength balance | Lower |
| Pitting Resistance | As much as 175% higher loads depending on offset | Lower |
| Scoring Resistance | Lower | As much as 200% higher loads |
| Sliding velocity | As much as 200% higher depending on the offset | Lower |
| Efficiency | As high as 96% depending on load and ratio | As high as 99% depending on load and ratio |
| Lubricant | EP (extreme pressure) | Mild EP |
| Sensitivity to misalignment | Varies with mounting rigidity and cutter diameter | Varies with mounting rigidity and cutter diameter |
| Manufacture | Larger point width cutter<br>Easier to lap | Smaller point width cutter<br>More difficult to lap |

| | | |
|---|---|---|
| Ratio | Better for high ratios | Better for low ratios |
| Position of vehicle centre of gravity | Lower drive shaft | Higher drive shaft |
| Outside Diameter of differential case | Smaller – due to less available space as a result of drive pinion interference | Larger – due to greater availability |
| Bearing reaction | Greater thrust on pinion | Less thrust on pinion |

Hypoid gears are very popular, especially for highway vehicles as they are even smoother and quieter than spiral bevel gears. One of the main attractions for the hypoid is relatively larger size of the hypoid pinion due to the offset. Even with the moderate offset, hypoid pinions are sufficiently larger to make practical considerably higher ratios in a single reduction. Hence, hypoid gears will be used in our design.

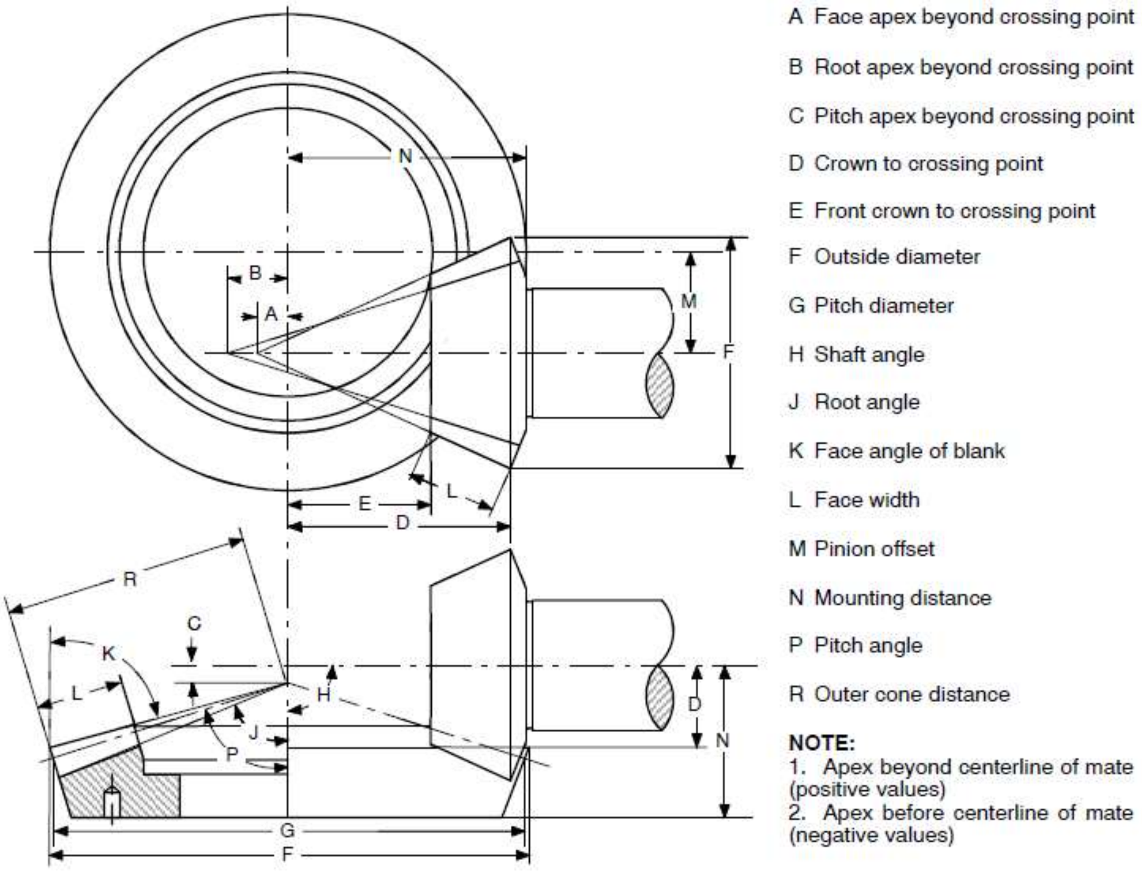


Figure 3.1: Hypoid gear nomenclature

### 3.2.2 Selection of drive gear size

## Gear loading

Analysing the characteristics of the load that would be imposed by the vehicle on the gears is not an easy task. This is due to operation at an inconsistence load. Also, some vehicles may need to run at higher loads.

## Performance Torque

This method of analysing the torque on the axle drive gears based on normal loads and overall vehicle performance has resulted in a more reliable estimate of the minimum gear sizes required for drive axles: (Thomas, 1984)

$$T_{PFG} = \frac{K_N W_C r_R}{100 N_D}(G_H + G_R)$$

Where (3.1)

$T_{PFG}$ =Performance torque (Nm),

$K_N$ =Unit conversion factor (for torque in Nm, $K_N$=9.807),

$W_C$ =Gross vehicle weight or gross combination weight (kg),

$r_R$ =Tire rolling radius,

$N_D$ =Number of driving axles,

$G_H$ =Highway grade factor, and

$G_R$ =Road rolling resistance factor.

Table 3.2: Gradeability

| **Type of vehicle** | **Gradeability, % (G)** |
|---|---|
| Domestic Highway Trucks | 3.5 – 7.0 |
| Foreign Highway Trucks | 5.0 – 9.0 |
| City Buses | 5.0 – 9.0 |
| Inter-urban Buses | 6.0 – 10.0 |
| Off- highway Trucks | 9.0 – 30.0 |
| Army Trucks | 5.0 – 9.0 |

Table 3.3: Road rolling resistance factors

| **Road Class** | **Road Surface Type** | **GR factor Condition of surface** | | |
|---|---|---|---|---|
| | | **Good** | **Fair** | **Poor** |
| I | Bituminous macadam (high type)<br>Cement concrete<br>Granite block<br>Asphaltic concrete<br>Wood block<br>Asphalt block<br>Brick | 1.00 | 1.10 | 1.20 |
| II | Oil mats (oiled macadam)<br>Bituminous macadam (low type)<br>Treated gravel<br>Bituminous (tar) | 1.20 | 1.60 | 2.00 |
| III | Crushed stones<br>Gravel<br>Cobbles<br>Sand-clay | 1.50 | 2.00 | 2.50 |
| IV | Sand<br>Earth | 2.00 | 2.50 | 3.50 |

## Prime Mover Torque

The axle torque based on maximum engine torque through low transmission ratio is the maximum theoretical value that can be developed by the automobile engine and then transferred to the wheels. However in actual practice it is seldom that this high torque with be applied.

The maximum gear torque resulting from the engine may be determined as follow: (Thomas, 1984)

$$T_{PMG} = \frac{K_O \, K_C \, T_E \, m_T \, m_c \, m_G}{N_D} \tag{3.2}$$

Where

$T_{PMG}$ =Maximum prime mover torque (Nm),

$K_O$ =Overload factor for shock loads resulting from snapping the clutch,

$K_C$ =unit conversion factor,

$T_E$ =Minimum net engine output torque (Nm),

$m_T$ =Transmission ratio in lowest gear (For highway trucks use value below 7, and for off highway application use highest transmission ratio employed more than 1% of the expected life),

$m_c$ =automatic transmission convertor ratio (For manual transmission, take mc =1),

$m_G$ =bevel or hypoid drive gear ratio used in the axle, and

$N_D$ =number of driving axle.

## Slip torque

Wheel slip torque is seldom a good measure for designing bevel gear for a highway vehicle. However for off highway applications it may become a limiting condition.

Maximum torque on the gear from slip of the wheels may be determined as follow: (Thomas, 1984)

$$T_{WSG} = \frac{K_N\ W_D\ f_s\ r_R\ M_G}{N_D M_A} \tag{3.3}$$

Where

$T_{WSG}$ = Maximum wheel slip torque (Nm),

$K_N$ = Unit conversion factor (=9.807 for torque in Nm),

$W_D$ = Loaded weight on driving axle = $W_L$ . $f_d$,

$W_L$ = Loaded weight of vehicle (kg) :GCW or GVW,

$f_d$ = Drive axle weight distribution factor (0.7-0.8 for GVW and 0.3-0.35 for GCW),

$f_s$ = Coefficient of friction between tires and road,

$r_R$ = Tire rolling radius (m),

$M_G$ = Bevel or hypoid gear ratio,

$N_D$ = Number of driving axles, and

$M_A$ = Overall axle ratio including bevel or hypoid drive gear, wheel reduction gear or two speed axle reduction gear.

## Estimated gear size

After calculation of performance torque, we can estimate the gear size for all vehicles using given graph:

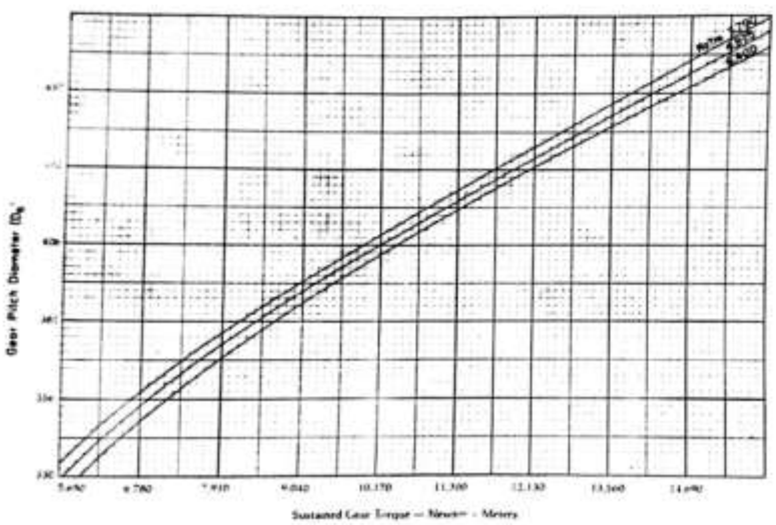

Figure 3.2: Charts for selecting approximate gear size for hypoid gears with 22.5° avg. pressure angle, 50 deg. pinion spiral angle, gear face width of approximately 28% of cone distance, and pinion offset approximately 11% of gear diameter (Thomas, 1984)

This graph is digitized by software named as 'Plot digitizer' from where these data points are taken. Plotting these data point on MATLAB, three equations for different gear ratios which are given below are generated:

For gear ratio = 3.7

$$D_G = 4.55E\text{-}11*(T_{PFG}^3) - 1.77E\text{-}6*(T_{PFG}^2) + (0.0353*T_{PFG}) + 184 \tag{3.4}$$

For gear ratio = 4.875

$$D_G = 5.41E\text{-}11*(T_{PFG}^3) - 2.11E\text{-}6*(T_{PFG}^2) + (0.0396*T_{PFG}) + 164 \tag{3.5}$$

For gear ratio = 6.4

$$D_G = 4.1E\text{-}11*(T_{PFG}^3) – 1.77E\text{-}6*(T_{PFG}^2) + (0.0371*T_{PFG}) + 164 \tag{3.6}$$

Interpolating them for desired gear ratio, preliminary gear diameter can be calculated. This interpolation calculation par is included in the excel calculation sheets. All the calculation sheets are attached along with the file.

Table 3.4: Specifications of the vehicle range for which tandem axle is to be designed

| **Vehicle** | | **Gear Box** | **GVW (T)** | **Overload Capacity (T)** | **Engine specifications** | | | | **FDR** |
|---|---|---|---|---|---|---|---|---|---|
| | | | | | **Power** | | **Torque** | | |
| | | | | | **(HP)** | **@rpm** | **(Nm)** | **@rpm** | |
| 6x4T 6025 | Onroad | 6s | 25 | 40 | 210 | 2200 | 825 | 1100-1700 | 5.83 |
| | | zf 9s | | | | | | | 5.83 |
| | | vecv 9s | | | | | | | 5.83 |
| | RMC | 6s | 25 | 40 | 210 | 2200 | 825 | 1100-1700 | 6.17 |
| | | zf 9s | | | | | | | 6.17 |
| | | vecv 9s | | | | | | | 6.17 |
| | Offroad | 6s | 25 | 40 | 210 | 2200 | 825 | 1100-1700 | 5.83 |
| | | zf 9s | | | | | | | 5.83 |
| | | vecv 9s | | | | | | | 5.83 |
| 6x4TT | TT | zf 9s | 49 | 63 | 250 | 2200 | 950 | 1100-1700 | 5.86 |
| | | vecv 9s | | | | | | | 5.86 |
| 8x4T | Tipper | zf 9s | 31 | 50 | 250 | 2200 | 950 | 1100-1700 | 5.86 |
| | | vecv 9s | | | | | | | 5.86 |
| | RMC | zf 9s | 40 | 40 | 250 | 2200 | 950 | 1100-1700 | 5.86 |
| | | vecv 9s | 40 | 40 | 250 | 2200 | 950 | 1100-1700 | 5.86 |
| V1 | Tipper | 9s | 25 | 40 | 280 | 2200 | 1050 | 1100-1700 | 5.57 |
| V2 | Tipper | 9s | 31 | 50 | 280 | 2200 | 1050 | 1100-1700 | 5.57 |
| V3 | TT | 9s | 49 | 60 | 280 | 2200 | 1050 | 1100-1700 | 5.57 |
| V4 | Tipper | 9s | 25 | 40 | 280 | 2200 | 1250 | 1100-1700 | 5.57 |
| V5 | Tipper | 9s | 31 | 50 | 280 | 2200 | 1250 | 1100-1700 | 5.57 |
| V6 | TT | 9s | 49 | 60 | 280 | 2200 | 1250 | 1100-1700 | 5.57 |

In the above table, T is a tipper truck, TT is tractor trailer and RMC is ready mix concrete truck. Similarly, 6s is speed transmission and 9s is nine speed transmission. ‘zf’ and ‘vecv’ are the transmission manufacturer’s name.

Initial calculations for all the vehicles for estimated gear diameters according to performance torque are calculated in the next table.

Table 3.5: Preliminary diameters for all the vehicles

| **Vehicle** | | **Gear Box** | **Crown gear diameter (DG) (mm)** | **Gear face width (FG) (mm)** | **Group** |
|---|---|---|---|---|---|
| 6x4T 6025 | Onroad | 6s | 348 | 53 | 1 |
| | | zf 9s | 348 | 53 | |
| | | vecv 9s | 348 | 53 | |
| | RMC | 6s | 349 | 53 | |
| | | zf 9s | 349 | 53 | |
| | | vecv 9s | 349 | 53 | |
| | Offroad | 6s | 390 | 59 | 2 |
| | | zf 9s | 390 | 59 | |
| | | vecv 9s | 390 | 59 | |
| 6x4TT | TT | zf 9s | 408 | 62 | |
| | | vecv 9s | 408 | 62 | |
| 8x4T | Tipper | zf 9s | 422 | 64 | |
| | | vecv 9s | 422 | 64 | |
| | RMC | zf 9s | 390 | 59 | |
| | | vecv 9s | 390 | 59 | |
| V1 | Tipper | 9s | 390 | 59 | |
| V2 | Tipper | 9s | 421 | 63 | |
| V3 | TT | 9s | 400 | 60 | |
| V4 | Tipper | 9s | 430 | 65 | 3 |
| V5 | Tipper | 9s | 430 | 65 | |
| V6 | TT | 9s | 430 | 65 | |

To pursue a modular design, three groups are made to divide the whole range. Now, we will calculate the bending and surface stresses and represent the values in a graph in next step.

### 3.2.3 Rating of Hypoid gears

Fundamental Bending and contacting stress formulae (Thomas, 1984):

The basic equation for the bending stress in a hypoid gear is

$$s_{tG} = \frac{2T_G K_o}{K_V} \cdot \frac{P_d}{F_G D} \cdot \frac{K_s K_m}{J_G} \tag{3.7}$$

And for the mating hypoid pinion is

$$s_{tP} = \frac{2T_P K_o}{K_V} \cdot \frac{P_d}{F_P D} \cdot \frac{N}{n} \cdot \frac{K_s K_m}{J_P} \tag{3.8}$$

Or

$$s_{tP} = \frac{2T_P K_o}{K_V} \cdot \frac{P_d}{F_G D} \cdot \frac{N}{n} \cdot \frac{K_s K_m}{J'_P} \tag{3.9}$$

The basic equation for the contact stress in a hypoid gear or pinion is

$$s_c = C_p \sqrt{\frac{2T_{Pmx} C_o}{C_V} \cdot \frac{1}{F_G D^2} \cdot \left(\frac{N}{n}\right)^2 \cdot \frac{C_s C_m C_f}{I}} \cdot \sqrt[3]{\frac{T_P}{T_{Pmx}}} \tag{3.10}$$

Where

$s_{tG}$ ,$s_{tP}$ = calculated tensile bending stresses at the root of the tooth for pinion and gear respectively,

$s_c$ = calculated contact stress at the point on tooth where its value will be maximum,

$C_p$ = elastic coeff. Of gear and pinion material combination ,

$T_P$, $T_G$ = transmitted torques of pinion and gear respectively,

$T_{Pmx}$ = maximum transmitted pinion torque,

$K_o$, $C_o$ = overload factors for strength and durability respectively,

$K_V$, $C_V$ = dynamic factors for strength and durability respectively,

$P_d$ = gear transverse diametral pitch at outer end of tooth, teeth/in.,

$F_P$, $F_G$ = face widths of pinion and gear respectively, mm,

D = gear outer pitch diameter, mm,

$n_N$ = numbers of teeth in pinion and gear respectively,

$K_s$, $C_s$ = size factors for strength and durability respectively,

$K_m$, $C_m$ = load distribution factors for strength and durability respectively,

$C_f$ = surface condition factor for durability,

$J_P$, $J_G$ = geometry factors for strength of pinion and gear respectively,

$J_P^{'}$ = modified pinion geometry factor for strength, and

I = geometry factor for durability.

The basic equation for working bending stress in a hypoid gear or pinion is (Thomas, 1984)

$$s_{wt} = \frac{s_{at}K_L}{K_T K_R}$$

(3.11)

The basic equation for working contact stress in a hypoid gear or pinion is (Thomas, 1984)

$$s_{wc} = \frac{s_{ac}C_L C_H}{C_T C_R}$$

Where (3.12)

$s_{wt}$, $s_{wc}$ = working tensile bending stress and working contact stress respectively, N/mm$^2$,

$s_{at}$, $s_{wc}$ = allowable tensile bending stress and allowable contact stress respectively, N/mm$^2$,

$K_L$, $C_L$ = life factors for strength and durability respectively,

$C_H$ = hardness ratio factor for durability,

$K_T$, $C_T$ = temperature factors for strength and durability respectively, and

$K_R$, $C_R$ = factors of safety for strength and durability respectively.

The material used in manufacturing of the gears is case carburised 20MnCr5. Using the same material, calculating factor of safeties for all the vehicles at different crown wheel diameter and analysing our results graphically will allow us to select gear specifications accordingly. Using above formulae and all the constants and other values from the source standards, following graphs can be made.

### Calculations for group 1:

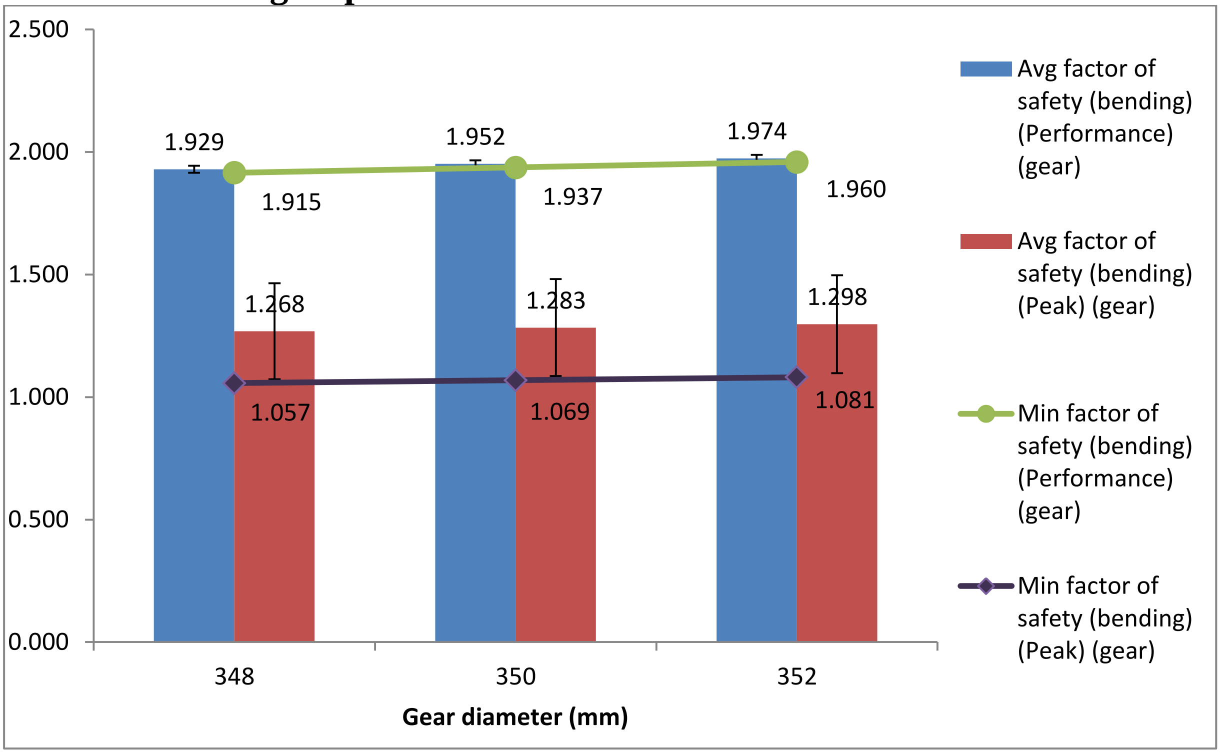


Figure 3.3: Factor of safety diagram for bending

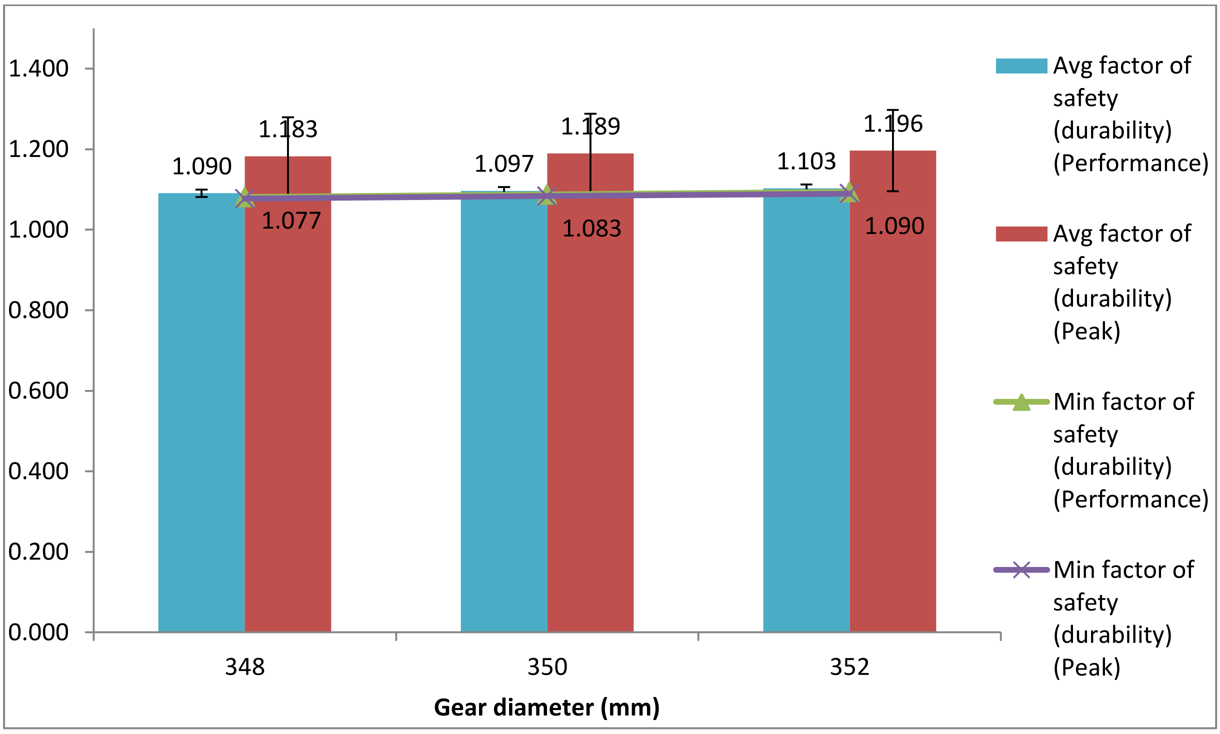


Figure 3.4: Factor of safety diagram for durability

## Calculations for group 2:

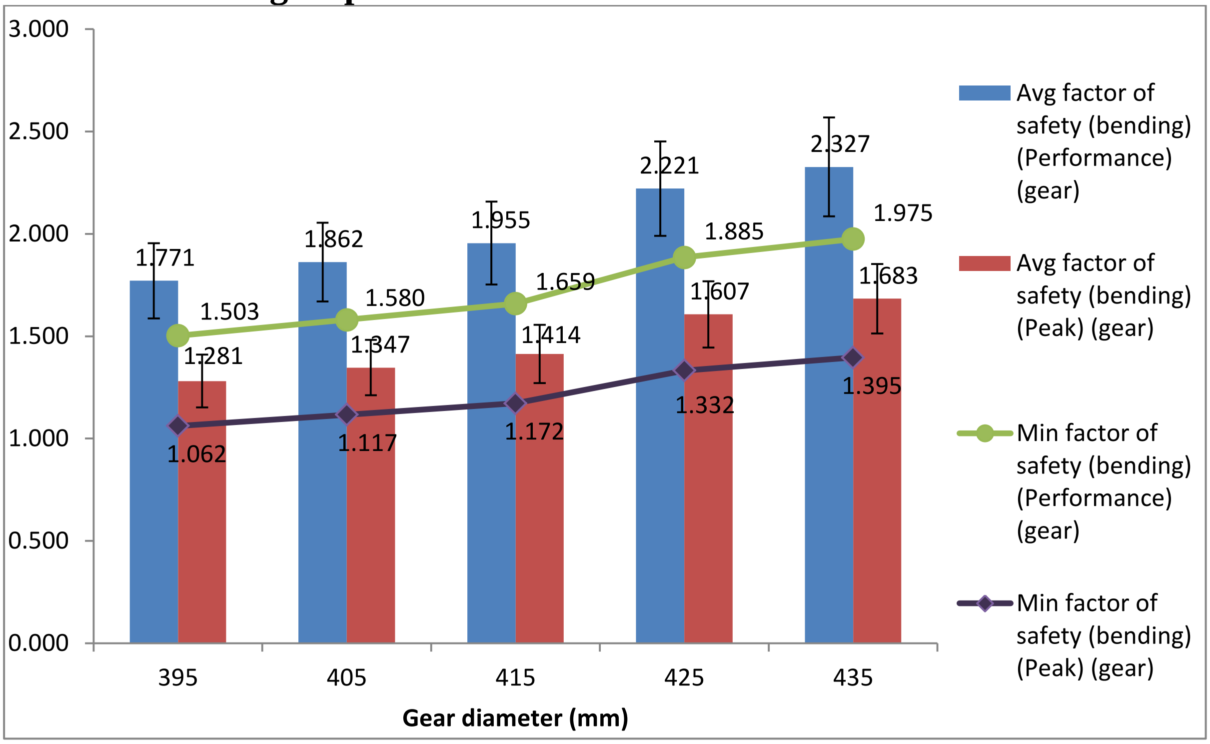


Figure 3.5: Factor of safety diagram for bending

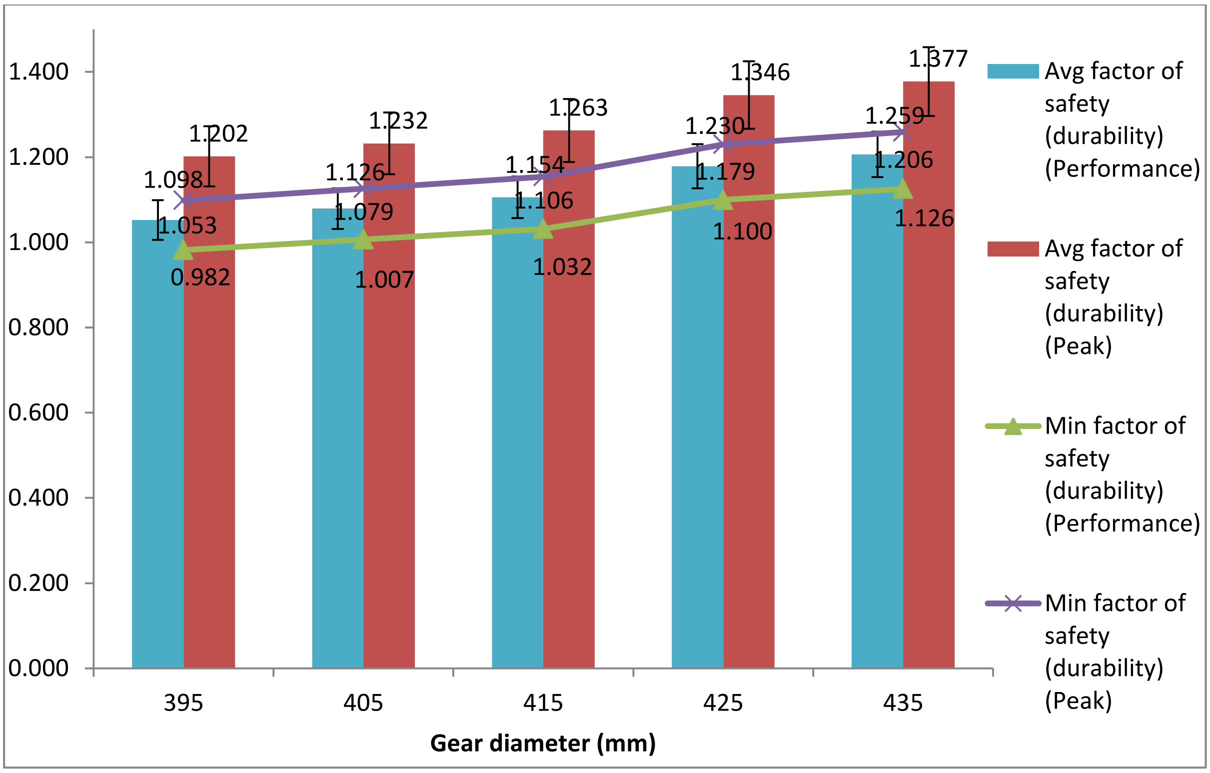


Figure 3.6: Factor of safety diagram for durability

## Calculations for group 3:

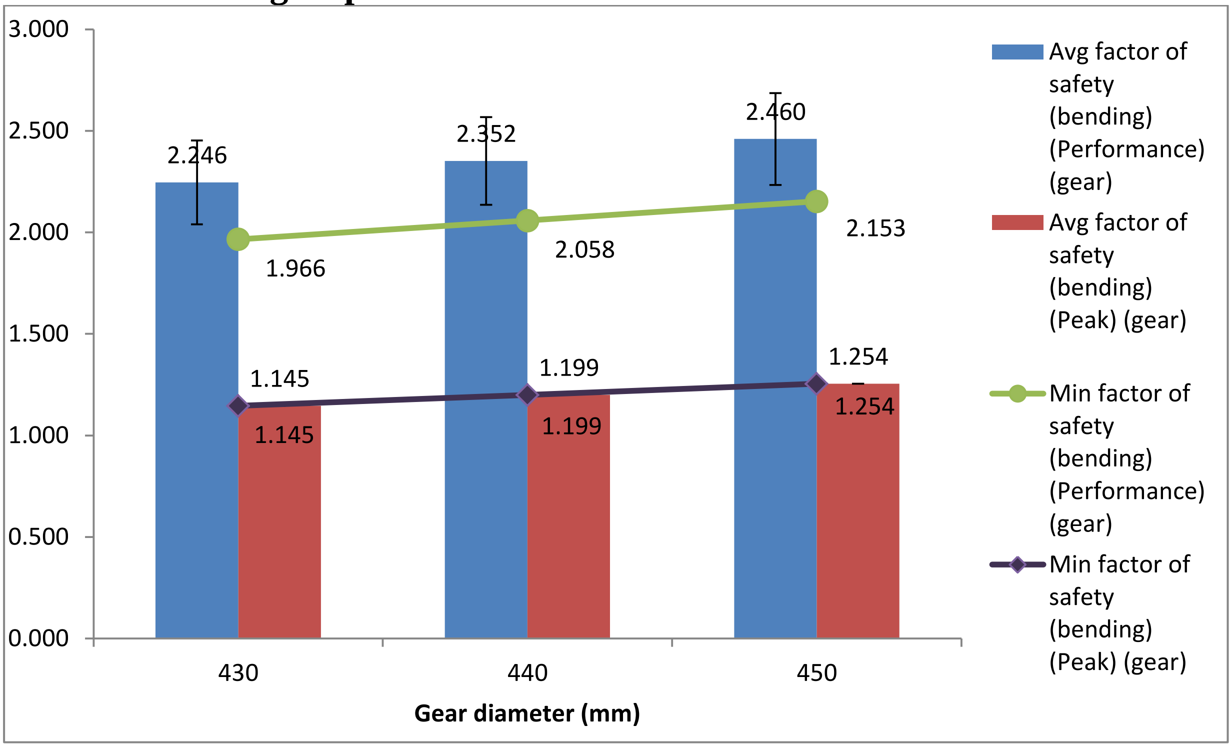


Figure 3.7: Factor of safety diagram for bending

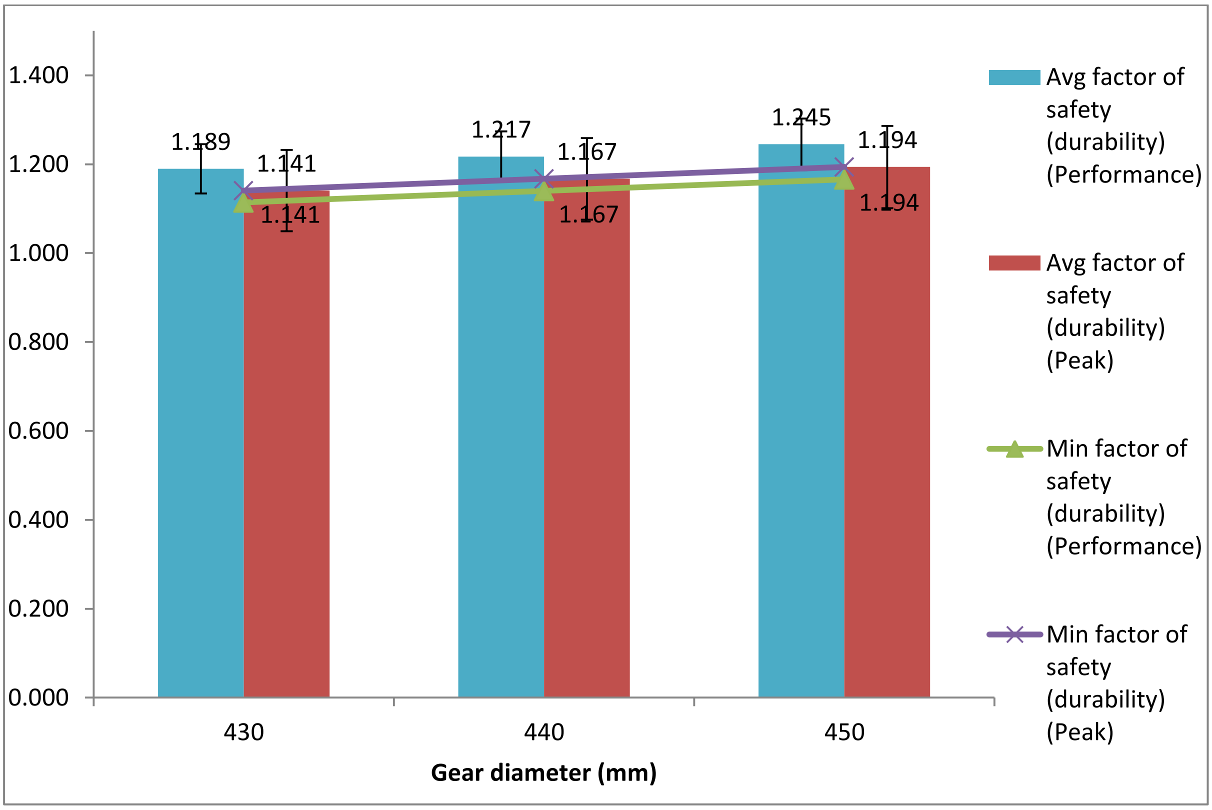


Figure 3.8: Factor of safety diagram for durability

Considering all these above graphs we may conclude following points:

- For group 1, estimated diameters for all the vehicles are coming out to be in same range (348-350 mm), therefore we may select a round off value of **350mm.**
- For group 2, the choice with depend on durability graph. Lowest case of factor of safety is seen in case of durability at performance loads therefore that will be our limiting condition. To be on a little safer side, we will select diameter of **415mm**, therefore, we may select this value. We are going with this minimum value of factor of safety of approximately 1 due to the fact that the vehicle is already designed at overload conditions.
- For group 3, estimated diameters are giving us sufficient values of factors of safety at minimum value, however hypoid gear set of 440 mm Drive head is already under production, so for modular design 440 mm diameter is selected.

All the selected diameters and face width (approximately 15% of diameter (Thomas, 1985)) will be input for Modular sheet, which will put them in final calculations sheet.

### 3.2.4 Hypoid Gear Specifications

After selecting preliminary gear diameter according to loading conditions, all other dimensions of hypoid gear pair are calculated according to **ANSI-AGMA 2005-D03** but prior to those following parameters must be decided:

- Gear ratio
- Hypoid pinion offset
- Hand of spiral

Minimum number of teeth on pinion maybe selected from following table:

Table 3.6: Suggested minimum numbers of pinion teeth (spiral and hypoid) (ANSI-AGMA 2005-D03)

| Approximate ratio | Minimum numbers of pinion teeth |
|---|---|
| 1.00 - 1.50 | 13 |
| 1.50 - 1.75 | 12 |
| 1.75 - 2.00 | 11 |
| 2.00 - 2.50 | 10 |
| 2.50 - 3.00 | 9 |
| 3.00 - 3.50 | 9 |
| 3.50 - 4.00 | 9 |
| 4.00 - 4.50 | 8 |
| 4.50 - 5.00 | 7 |
| 5.00 - 6.00 | 6 |
| 6.00 - 7.50 | 5 |
| 7.50 - 10.0 | 5 |

Calculation program for all the parameters of a hypoid gear pair according to 'Design of bevel gear ANSI-AGMA 2005-D03'is made in MS Excel. The program includes an iteration process which is done using the macro feature.

All of the calculation sheets can be found attached with the file **(Appendix B)** while formulae used could be found in **Appendix A**. However, sample calculations for the specifications of hypoid gear set for 8x4TT are as follows.

Table 3.7: Calculation sheet for hypoid specifications

| **Hypoid design formula(ALL ANGLES IN RADIANS)** | | | | |
|---|---|---|---|---|
| **Item** | | **Pinion** | **Both Pinion And Gear** | **Gear** |
| Pitch diameter | | 70.853 | | 415.00 |
| No of teeth | n, N | 7.000 | | 41.00 |
| Gear ratio | mG | | 5.857 | |

| | | | | | | | |
|---|---|---|---|---|---|---|---|
| Offset | E | | 44.45 | | | | |
| Pinion Spiral angle selected | ψP | 47.00 | | | | | |
| Cutter radius | rc | | 152.40 | | | | |
| | | | | | | | |
| Pressure angle (rad) | ϕ | | 0.3927 | | | | |
| Desired pinion spiral angle, | ψoP | 0.82030 | | | | | |
| module | met | | 10.12195 | | | | |
| Tooth taper | | | standard depth taper | | | | |
| Shaft angle | Σ | | 1.57080 | | | | |
| Shaft angle departure from 90 deg. | ΔΣ | | 0.00000 | | | | |
| Approximate gear pitch angle, | Γi | | | 1.36871 | | | |
| Face width | FG | | | 65.00000 | | | |
| Gear mean pitch radius | R | | | 175.66135 | | | |
| Approximate pinion offset angle in pitch plane | ε'2i | 0.25051 | | | | | |
| Approximate hypoid dimension factor | K1 | | 1.23462 | | | | |
| Approximate pinion mean radius | R2P | 37.02748 | | | | | |
| **Iterative process** | | | | | | | |
| Initial Assumption | | | | | Angles in deg. | | |
| Gear offset angle in axial plane | η | | | 0.05380 | | | 3.083 |
| Iteration process | | | | | | | |
| Gear offset angle in axial plane | η | | | 0.0538 | | | 3.083 |
| Intermediate pinion offset angle in axial plane | ε2 | 0.2441 | | | 13.987 | | |
| Intermediate pinion pitch angle | γ2 | 0.2126 | | | 12.183 | | |

| | | | | | | | |
|---|---|---|---|---|---|---|---|
| Intermediate pinion offset angle in pitch plane | ε′2 | 0.2499 | | | 14.316 | | |
| intermediate pinion mean spiral angle | ψ2P | 0.8213 | | | 47.054 | | |
| increment in hypoid dimension factor | ΔK | | -0.0005 | | | | |
| Ratio of pinion mean radius increment to gear mean pitch radius | ΔRP/R | | -0.0001 | | | | |
| pinion offset angle in axial plane | ε1 | 0.2441 | | | 13.988 | | |
| pinion pitch angle | γ | 0.2126 | | | 12.182 | | |
| pinion offset angle in pitch plane | ε′1 | 0.2499 | | | 14.317 | | |
| Spiral angle | ψP, ψG | 0.8203 | | 0.5704 | 47.000 | | 32.683 |
| Gear pitch angle | Γ | | | **1.3516** | | | 77.439 |
| mean cone distance | AmG | | | 179.9686 | | | |
| Pinion mean radius increment | ΔRP | -0.0151 | | | | | |
| mean cone distance | AmP | 175.3952 | | | | | |
| Mean pinion radius | RP | 37.0123 | | | | | |
| Limit pressure angle | ϕo | | -0.0368 | | | -2.106 | |
| Mean tooth curvature | | | | | | | |
| | | | | | | | |
| | | | | | | | |
| | | | | | | | |
| | | | | | | | |
| | ρ | | 152.4000 | | | | |
| Hypoid radius of curvature | rc1 | | 152.3994 | | | | |
| Iteration factor | Δ | | 0.0000 | | | | |
| | | | True | | | | |
| Pressure angle concave | ϕ1, ϕ2 | 0.3559 | | 0.4295 | 20.394 | | 24.606 |
| Pressure angle convex | ϕ2, | 0.4295 | | 0.3559 | 24.606 | | 20.39 |

| | | | | | | | |
|---|---|---|---|---|---|---|---|
| | φ1 | | | | | | 4 |
| crossing point to mean point along gear axis | ZG | | 36.9588 | | | | |
| Gear pitch apex beyond crossing point | Z | | | 2.1792 | | | |
| Outer cone distance | AoG | | | 212.5879 | | | |
| Gear face width from calculation point to outside | ΔFo | | | 32.6193 | | | |
| Equivalent 90 deg. Ratio | m90 | | 4.4883 | | | | |
| Depth factor (table 4) | k1 | | 1.8350 | | | | |
| Mean addendum factor (table 5) | c1 | | 0.1179 | | | | |
| Mean working depth | h | | 13.2343 | | | | |
| Mean addendum | aP, aG | 11.6734 | | 1.5609 | | | |
| Clearance factor | k2 | | 0.1250 | | | | |
| Mean dedendum | bP, bG | 3.2152 | | 13.3277 | | | |
| Clearance | c | | 1.6543 | | | | |
| Mean whole depth | hm | | 14.8886 | | | | |
| Sum of dedendum angles(table 6) | Σδ | | 0.0918 | | | 5.259 | |
| Dedendum angle | δG | | | 0.0739 | | | 4.235 |
| Addendum angle | αG | | | 0.0179 | | | 1.023 |
| Outer addendum | aoG | | | 2.1435 | | | |
| Outer dedendum | boG | | | 15.7368 | | | |
| Gear whole depth | htG | | | 17.8803 | | | |
| Outer working depth | hk | | 16.2260 | | | | |
| Root angle | ΓR | | | 1.2777 | | | 73.20 4 |
| Face angle | Γo | | | 1.3694 | | | 78.46 3 |
| Gear outside diameter | Do | | | 415.9323 | | | |
| Gear crown to crossing point | Xo | | | 41.9603 | | | |
| Root apex beyond crossing point | ZR | | | 2.1411 | | | |

| | | | | | | | |
|---|---|---|---|---|---|---|---|
| Face apex beyond crossing point | Zo | | | 0.4913 | | | |
| Auxiliary angle for calculating pinion offset angle in root plane | ζR | 0.0000 | | | 0.000 | | |
| Auxiliary angle for calculating pinion offset angle in face plane | ζo | 0.0000 | | | 0.000 | | |
| Pinion offset angle in root plane | εR | 0.2402 | | | 13.765 | | |
| Pinion offset angle in face plane | εo | 0.2451 | | | 14.041 | | |
| Face angle | γo | 0.2845 | | | 16.300 | | |
| Root angle | γR | 0.1953 | | | 11.188 | | |
| Face apex beyond crossing point | Go | -2.3087 | | | | | |
| Root apex beyond crossing point | GR | 0.1097 | | | | | |
| Addendum angle | αP | 0.0719 | | | 4.118 | | |
| Dedendum angle | δP | 0.0174 | | | 0.994 | | |
| Angle between projection of pinion axis into pitch plane and pitch element | λ′ | 0.0091 | | | 0.519 | | |
| Gear face width from calculating point to inside | ΔFi | | | 32.3807 | | | |
| Pinion face width increment | ΔFoP | 2.6113 | | | | | |
| Pinion face width from a calculating point to outside | FoP | 33.5872 | | | | | |
| Pinion face width from calculating point to inside | FiP | 33.3414 | | | | | |
| Incerment along pinion axis from calculating point to | ΔBo | 32.4685 | | | | | |

| | | | | | | | |
|---|---|---|---|---|---|---|---|
| outside | | | | | | | |
| Increment along pinion axis from calculating point to inside | ΔBi | 37.1587 | | | | | |
| Crown to crossing point | xo | 202.921<br>1 | | | | | |
| Front crown to crossing point | xi | 133.293<br>9 | | | | | |
| Whole depth, pinion | htP | | | | | | |
| Outside diameter | do | 117.325<br>4 | | | | | |
| Face width | FP | 72.5431 | | | | | |
| Mean circular pitch | pm | | 26.9198 | | | | |
| Mean diametral pitch | Pdm | | 0.1167 | | | | |
| Thickness factor | k3 | | 0.1349 | | | | |
| Mean pitch diameter | dm,<br>Dm | 74.0247 | | 351.3227 | | | |
| Pitch diameter | d | 89.3329 | | | | | |
| Mean normal circular tooth thickness, theoretical without backlash | tn,<br>Tn | 12.1922 | | 6.1672 | | | |
| Outer normal backlash allowance (from table) | B | | 0.4100 | | | | |
| Outer gear spiral angle face milling | ψoG | | | 0.7139 | | | 40.90<br>1 |
| Mean normal chordal tooth thickness | tnc,<br>Tnc | 11.9684 | | 5.9982 | | | |
| Mean chordal addendum | acp,<br>acG | 12.1641 | | 1.5668 | | | |

## 3.2.5 Hypoid geometry

Complete calculation of hypoid geometry becomes very complex at times. All the above dimensions calculated in above table may be understood with the help of the following diagrams.

Figure 2.10 shows the major angles and quantities involved. Figure 2.10(A) is a side view looking along the pinion axis. Figure 2.10(B) is a front view looking along the gear axis. Figure 2.10(C) is a top view showing the shaft angle between the gear and pinion axes. Figure 2.10(D) is a view of the gear section along the plane making the offset angle, ε, in the pinion axial plane. Figure 2.10(E) is a view of the pitch plane; *T*. Figure 2.10(F) is a view of the pinion section along the plane making the offset angle, η, in the gear axial plane. Figure 2.10(G) is a view of the pitch plane, *T*. [Annexure D, ANSI-AGMA 2005-D03]

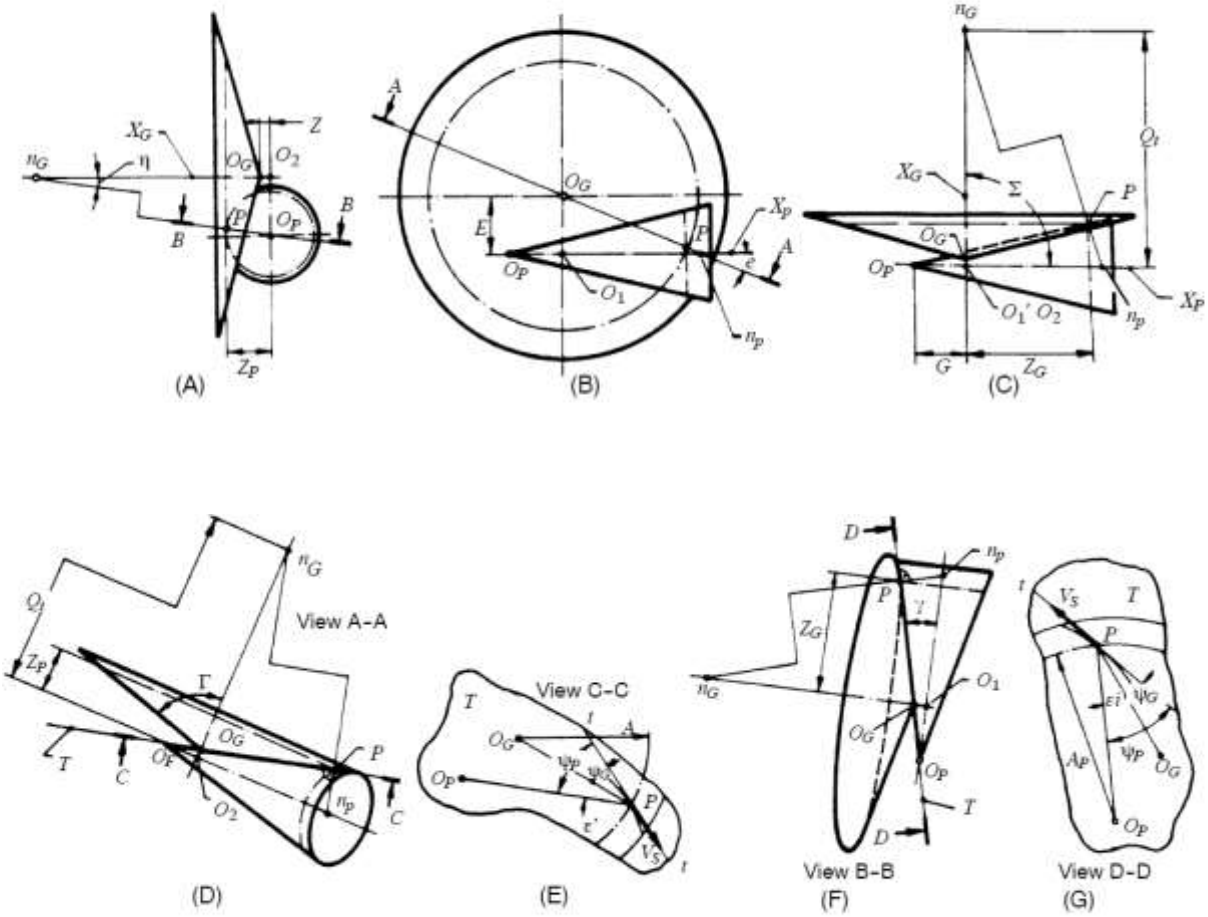


Figure 3.9: Hypoid geometry

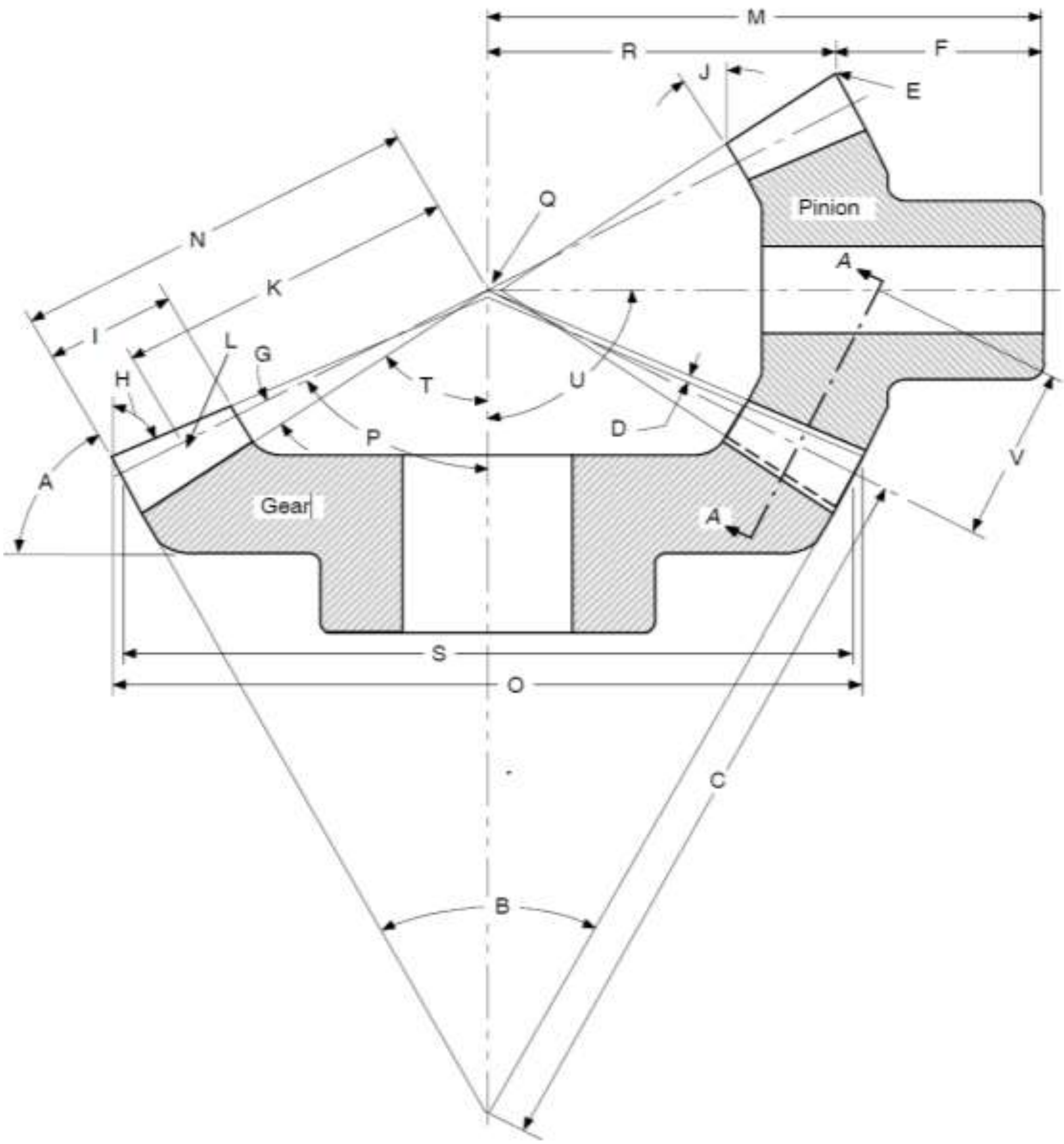


| | | | | | |
|---|---|---|---|---|---|
| A | Back angle | H | Face angle | P | Pitch angle |
| B | Back cone angle | I | Face width | Q | Pitch cone apex |
| C | Back cone distance | J | Front angle | R | Pitch cone apex to crown |
| D | Clearance | K | Mean cone distance | S | Pitch diameter |
| E | Crown point | L | Midface | T | Root angle |
| F | Crown to back | M | Mounting distance | U | Shaft angle |
| G | Dedendum angle | N | Outer cone distance | V | Equivalent pitch radius |
| | | O | Outside diameter | | |

Figure 3.10: Bevel gear nomenclature - axial plane

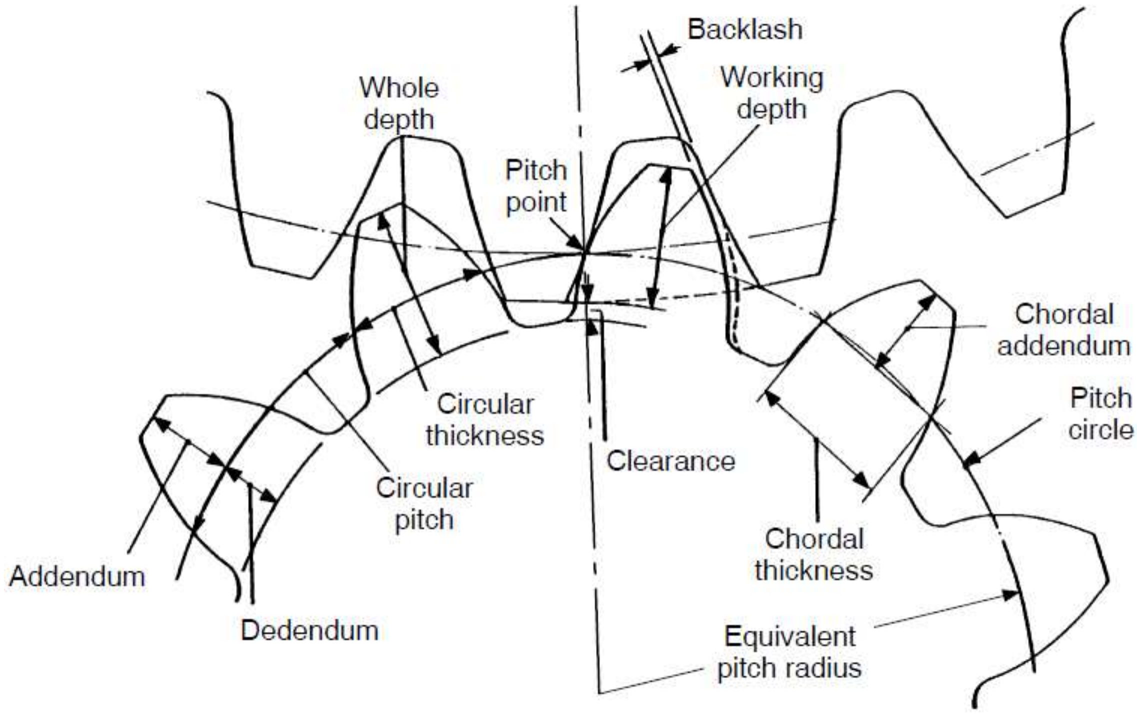


Figure 3.11: Bevel gear nomenclature -- mean section (A-A in figure 11)

### 3.2.6 Significance of Depth factor, mean addendum factor and clearance factor

## Depth factor, $k_1$

Depth factor plays a significant role in bevel gear geometry as it decides mean working depth of the gear teeth. Normally a depth factor, $k_1$, of 2.000 is used to calculate **mean working depth, *h***, but it can be varied to suit design and other requirements. A table is provided in ANSI-AGMA 2005-D03 for suggested values for depth factor based on no of teeth in pinion. As the number of teeth on pinion decreases, depth factor also decreases.

## Mean addendum factor, $c_1$

This factor divides the working depth between the pinion and gear addendums. The pinion addendum is longer than the gear addendum, except when the numbers of teeth are equal. Longer addendums are used on the pinion as to avoid undercut. A table is given in ANSI-AGMA 2005-D03 for suggested values for mean addendum factor based on no of teeth in pinion. Other values based on sliding velocity, top land or point width limits, or matching strength between two members, can be used.

## Clearance factor, $k_2$

While the clearance is constant along the entire length of the tooth, the calculation is made at midface. Normally the value of 0.125 is used for the clearance factor, $k_2$, but it can be varied to suit the design and other requirements.

## Mean working depth, h

The depth calculation is made at midface to assure proper depth of contact at this section of the tooth for any depth wise taper. Working depth can be seen above in figure 3.11.

$$\text{working depth, } h = \frac{2k_1 R \cos\psi_G}{N} \tag{3.13}$$

Where

R = Gear mean pitch radius

N = Number of teeth on the gear3

$\psi_G$ = Spiral angle of the gear

## Mean addendum, $a_P$ and $a_G$

After calculation of mean working depth, mean addendum factor apportions it into pinion and gear addendums with following relations.

$$a_G = c_1 h \tag{3.14}$$

$$a_P = h - a_G = h(1 - c_1) \tag{3.15}$$

## Mean dedendum, $b_P$ and $b_G$

$$b_G = h(1 + k_2 - c_1) \tag{3.16}$$

$$b_P = b_G + a_G - a_P = h(k_2 + c_1) \tag{3.17}$$

## Mean whole depth, $h_m$

Mean whole depth defines the total tooth length of the gear in contrast to the mean working depth which tells us about the tooth length coming in contact with each other.

$$h_m = a_G + b_G = h(1 + k_2) \tag{3.18}$$

### 3.2.7 Analysis of forces [ANSI-AGMA 2005-D03]

The gear tooth forces are tangential, axial and radial. The axial and radial forces are dependent on the curvature of the loaded tooth face.

In figure 3.12 (A), the forces are due either to a right-hand crown wheel being driven counter clockwise or driving clockwise, or to a left-hand crown wheel being driven clockwise or driving counter clockwise.

In figure 3.13 (A), the forces are due either to a right-hand crown wheel being driven clockwise or driving counter clockwise, or to a left-hand crown wheel being drive counter clockwise or driving clockwise.

In figure 3.12 (B), the forces are due either to a left-hand pinion driving clockwise or being driven counter clockwise, or to a right-hand pinion driving counter clockwise or being driven clockwise.

In figure 3.13(B), the forces are due either to a left-hand pinion driving counter clockwise or being driven clockwise, or to a right-hand pinion driving clockwise or being driven counter clockwise.

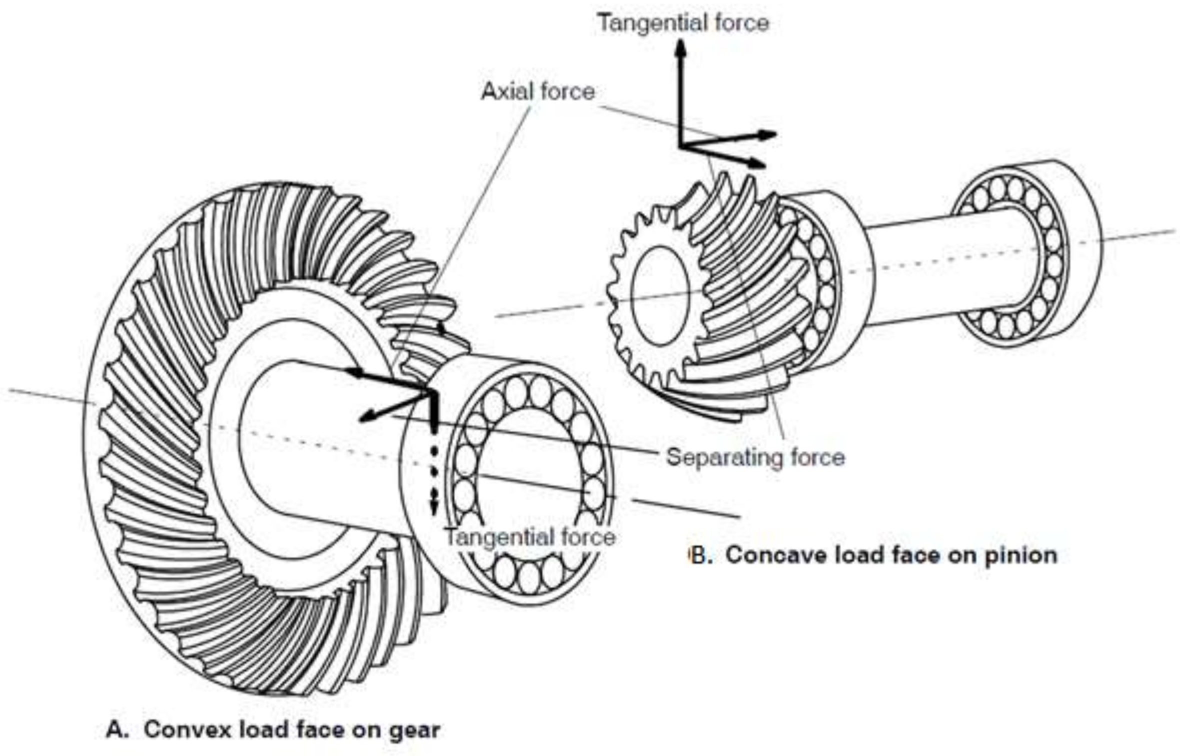


Figure 3.12: Resultant gear tooth forces

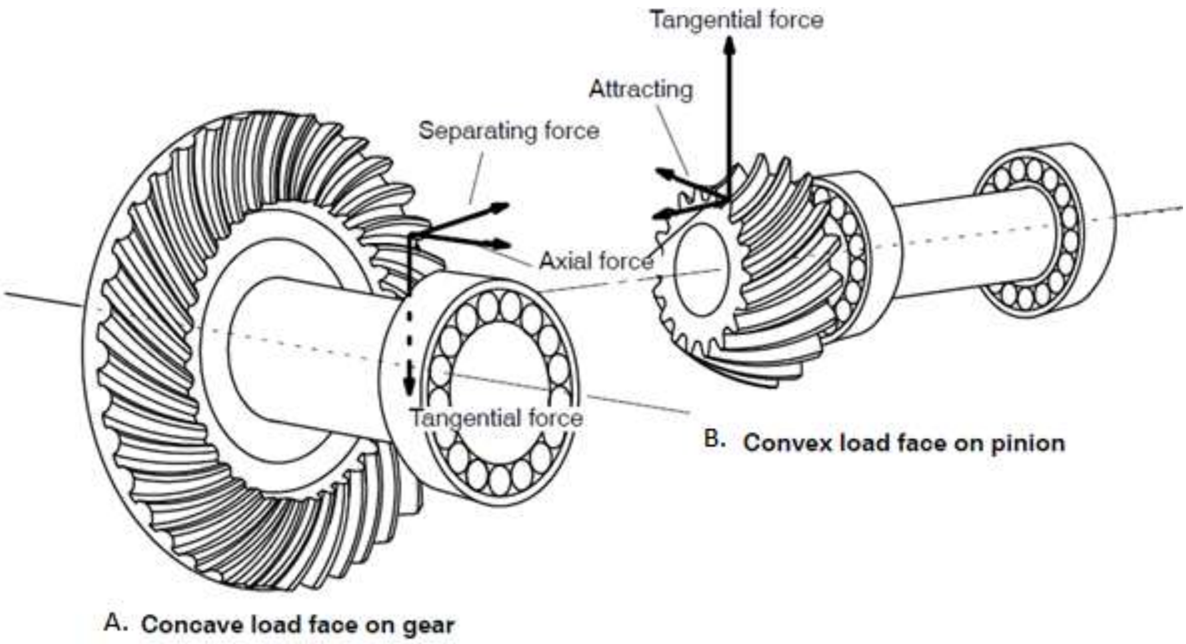


Figure 3.13: Resultant gear tooth forces

Below table is used to determine the load face.

Table 3.8: Relationship between load face and hand of the pinion

| Pinion hand of spiral | Rotation of driver | Load face | |
|---|---|---|---|
| | | Driver | Driven |
| Right | Clockwise | Convex | Concave |
| | Counter clockwise | Concave | Convex |
| Left | Counter clockwise | Concave | Convex |
| | Clockwise | Convex | Concave |

## Tangential

The tangential force on a bevel gear (member with larger number of teeth) is given by:

$$W_{tG} = \frac{2T_G}{D_m} \tag{3.19}$$

Where, $W_{tG}$ = is tangential force at mean diameter on the gear, N;

$T_G$ = is torque transmitted by the gear, Nm.

The tangential force on the mating pinion is given by:

$$W_{tP} = \frac{2T_P}{d_m} \quad (3.20)$$

Where, $W_{tP}$ = is tangential force at mean diameter on the gear, N;

$T_P$ = is torque transmitted by the gear, Nm.

## Axial

The values of axial force, $W_x$, on bevel gears are given in the following formulas. The symbols in the formulas represent the values (e.g., tangential force, spiral angle, pitch angle, and pressure angle) for the gear or pinion member under consideration:

For a concave load face:

$$W_x = \frac{W_t}{\cos\psi}(\tan\phi\sin\gamma + \sin\psi\cos\gamma) \quad (3.21)$$

For a convex load face:

$$W_x = \frac{W_t}{\cos\psi}(\tan\phi\sin\gamma - \sin\psi\cos\gamma) \quad (3.22)$$

Where, $W_x$ = Axial force, N;

$W_t$ = Tangential force, N;

$\phi$ = Normal pressure angle. This is the pressure angle on the loaded side of the tooth (depending upon direction of rotation);

$\gamma$ = Pitch angle of pinion or gear on bevel gears.

A positive sign (+) indicates direction of thrust is away from pitch apex.

A negative sign (-) indicates direction of thrust is toward pitch apex.

## Radial

The values of radial force, $W_r$, on bevel gears are given in the following formulas. When using the formulas the tangential force, spiral angle, pitch angle, and pressure angle of the corresponding member must be used:

For a concave load face:

$$W_r = \frac{W_t}{\cos\psi}(\tan\phi\cos\gamma + \sin\psi\sin\gamma) \quad (3.23)$$

For a convex load face:

$$W_r = \frac{W_t}{\cos\psi}(\tan\phi\cos\gamma - \sin\psi\sin\gamma) \tag{3.24}$$

Where; $W_r$ = Radial force, N.

A positive sign (+) indicates direction of force is away from the mating member. This is commonly called the separating force. A negative sign (-) indicates direction of force is toward the mating member. This is commonly called the attracting force.

## 3.3 Helical Gears

Helical gear in tandem axle is required to transfer the power from the IAD to the pinion of the differential of the first axle. The preliminary design procedure followed to design this helical gear is referred from Venkatesh et al., 2010. The desired torque and power output will be same as of the pinion input; therefore it will be designed at the same conditions. To design a helical gear be have to provides inputs like torque, power, speed, helix angle. Full length involute teeth with normal pressure angle of 20° are considered for this application. After designing the gear pair, ratings of both pitting resistances and bending strength are calculated.

From the calculations of hypoid gear, we could observe that maximum performance and peak torques on pinion for all the 3 groups in chapter 2 are as follow:

Table 3.9: Maximum pinion torque values

| | Maximum performance torque (Nm) | Maximum peak torque (Nm) |
|---|---|---|
| Group 1 | 1140 | 2784 |
| Group 2 | 2067 | 4242 |
| Group 3 | 2067 | 5050 |

In our pursuit of achieving a modular design, only one helical gear pair will be designed. Therefore, we will design a helical gear pair for group 3 which will be a safe design for all the groups.

### 3.3.1 Design Methodology
**(Venkatesh et al., 2010)**:

1. Gear design almost always starts with the selection of material. Proper material selection is very important. The material used is alloy steel 20MnCr5 with case hardened and then tempered.
2. Find out the minimum central distance based on the surface compression stress is:

$$a \geq (i+1)\sqrt[3]{\left(\frac{0.7}{[\sigma_c]}\right)^2 \frac{E\,[M_t]}{i.\Psi}} \tag{3.25}$$

Where:

| | | |
|---|---|---|
| $a$ | = | Centre distance |
| $i$ | = | Gear ratio |
| $[\sigma_c]$ | = | Design Surface stress or contact |
| $E$ | = | Equivalent Young's modulus |
| $[M_t]$ | = | $M_t.k_d.k$ |
| $M_t$ | = | torque transmitted by the pinion |
| $k_d$ | = | Dynamic load factor |
| $k$ | = | Load concentration factor |
| $\Psi$ | = | b/a |
| $b$ | = | Face width |

3. Minimum normal module may be determined as:

$$m_n \geq 1.15 \cos\beta * \sqrt[3]{\frac{[M_t]}{y_v[\sigma_b]\Psi_m Z_P}} \tag{3.26}$$

Where:

| | | |
|---|---|---|
| $Z_P$ | = | Assumed no of teeth on pinion |
| $\Psi_m$ | = | $b/m_n$ |
| $[\sigma_b]$ | = | Design bending stress (tensile) |
| $\beta$ | = | Helix angle, about 8° to 25° for helical, assumed 25° |
| $y_v$ | = | Form factor based on equivalent number of teeth on virtual cylinder, $Z_v$ |
| $Z_v$ | = | $Z/\cos^3\beta$ for helical gears |

Now, pinion dia, $D_P = m_n \frac{Z_P}{\cos\beta}$, gear dia, $D_G = m_n \frac{Z_G}{\cos\beta}$

Centre to centre distance, $a = \frac{D_1+D_2}{2}$ and face width, $b = \Psi . a$

4. To check if our design is valid:
   a. based on the contact stresses,

$$\sigma_c = 0.7 * \frac{i+1}{a} * \sqrt{\frac{i+1}{i*b} * E * [M_t]} \tag{3.27}$$

   b. based on the bending strength,

$$\sigma_b = 0.7 * \frac{i+1}{a* b* m_n * y_v} * [M_t] \tag{3.28}$$

As the values obtained for bending and contact stresses are less than the values of the material, the design is safe i.e. $\sigma_c \leq [\sigma_c]$ and $\sigma_b \leq [\sigma_b]$.

Since, as the space constraint has to be considered, design can be optimised by varying number of teeth, normal module and further face width by changing $\Psi$, if needed. Once, these thing s are optimised, gears' specifications can be calculated using following relationships:

Table 3.10: Standard tooth proportion for helical gears

| | |
|---|---|
| Tooth addendum, a | $1.00\, m_n$ |
| Tooth dedendum, b | $1.25\, m_n$ |
| Pinion pitch diameter | $\frac{Z_P m_m}{\cos \Psi}$ |
| Gear pitch diameter | $\frac{Z_G m_m}{\cos \Psi}$ |
| Pinion base diameter | $D_P \cos \phi_t$ |
| Gear base diameter | $D_G \cos \phi_t$ |
| Standard centre distance | $\frac{D_P + D_G}{2}$ |
| Pinion outside diameter | $D_P + 2a$ |
| Gear outside diameter | $D_G + 2a$ |
| Pinion root diameter | $D_P - 2b$ |
| Gear root diameter | $D_G - 2b$ |

### 3.3.2 Force Analysis

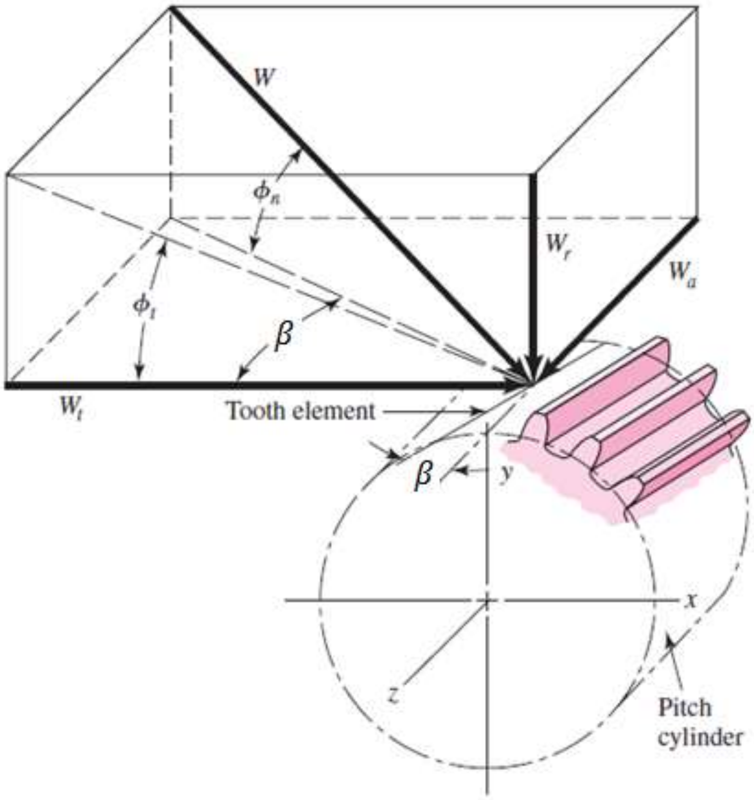


Figure 3.14: Tooth forces on a right hand helical gear

3-D view of the forces acting against a helical gear tooth is represented in figure 3.14. The point of application of the forces is in the pitch plane and in the centre of the gear face. From the figure, the 3 components of the total normal forces on the tooth are:

$$W_r = W * \sin \phi_n \quad (3.29)$$

$$W_t = W * \cos \phi_n * \cos \beta \quad (3.30)$$

$$W_a = W * \cos \phi_n * \sin \beta \quad (3.31)$$

Where: $W$ = force (total)

$W_r$ = radial component of the force

$W_t$ = tangential component of the force

$W_a$ = axial component of the force

$\phi_n$ = Normal pressure angle

$\beta$ = Helix angle

*As* value of $W_t$ is commonly known, other forces may be evaluated as:

Dividing (1) by (2), $\frac{W_r}{W_t} = \frac{\tan \phi_n}{\cos \beta} = \tan \phi_t$

We can observe from the figure, $\tan \phi_n = \tan \phi_t \cos \beta$

So, $$W_r = W_t \tan \phi_t \tag{3.32}$$

Now, dividing (3) by (2), $\frac{W_a}{W_t} = \tan \beta$

So, $$W_a = W_t \tan \beta \tag{3.33}$$

Also, rearranging (2), $$W = \frac{W_t}{\cos \phi_n \cos \beta} \tag{3.34}$$

### 3.3.3 Lewis and Buckingham equation analysis for dynamic loads

All the equations used to design assume the load to be static. However when the gear is running at high speeds, concept of dynamic loading comes into play. To account for this effect, $C_v$ (dynamic or velocity factor) developed by Barth comes into play. Now velocity factor further depends on pitch line velocity. For velocity ranging between 5-20 m/s, $C_v = \frac{6+v_m}{6}$ where vm is pitch line velocity in m/s.

Therefore design tangential force including dynamic effect, $F_D = F_t \times C_v$

For safe design, this FD should be less than beam strength of gear tooth which is given by Lewis equation:

$$F_s = [\sigma_b] * b * \pi * m_n * y_v \tag{3.35}$$

During power transmission through gears, because of inaccuracies of the tooth profile and gear tooth deflection under loads, gear teeth are also subjected to dynamic loading. Buckingham derived a dynamic load equation to use in such situations for finding out the highest load acting on the tooth, which is $F_D = F_t + F_i$, Where $F_D$ = Maximum dynamic load, $F_t$ = Static load produced by the power, $F_i$ = Incremental load due to dynamic action, Incremental load depends on the pitch line velocity, face width, of a gear tooth, gear materials, accuracy of cut and the tangential load and is given by

$$F_D = F_t + \left[\frac{0.164\, V_m \left(c\, b\, \cos^2 \beta + F_t\right) \cos \beta}{0.164\, V_m + 1.485 \sqrt{c\, b\, \cos^2 \beta + F_t}}\right] \tag{3.36}$$

In this equation, $V_m$ = Pitch line velocity in m/min, b = Face width of the gear tooth in mm, c = Dynamic factor (or) Deformation factor in N/mm. Deformation factor "C", Value of depends on tooth form and material of pinion and gear and can be found via a table from design data.

Apart from bending stresses, pitting is another major reason for the failure of gears. This failure happens when the contact stresses amongst the two meshed teeth surpasses the limit value of the material known as surface endurance. To avoid such failures, the dimensions of gear teeth and the material surface properties such as surface hardness should be designated in a way that the durability of the gear teeth are more than the effective load between the meshing teeth.

Based on Hertz theory of contact stresses, Buckingham derived an equation for durability of gear teeth that is:

$$\text{Limiting load for wear (N)}, F_w = \frac{b\,d\,Q\,k}{\cos^2\beta} \quad (3.37)$$

Where,

$$k = [\sigma_c{}^2]\frac{\sin\alpha_n}{1.4}\left[\frac{1}{E_1}+\frac{1}{E_2}\right]$$

$$Q, \text{Ratio factor} = \frac{2\,i}{i+1} \text{ where } i = \text{gear ratio}$$

$$d = \text{pitch circle diameter of pinion (mm)}$$

$$b = \text{Face width of the pinion (mm)}$$

For gear to be safe, following relations are to be true, $F_s \geq F_D$ and $F_w \geq F_D$.

## Design calculations

An excel calculation sheet is generated to for the calculations. Sample calculations are as follows:

| | | | |
|---|---|---|---|
| Pinion Torque Performance | Mt | 2067000 | Nmm |
| Pinion Torque Peak | Mtp | 5050000 | Nmm |
| Dynamic load factor | kd | 1.3 | |
| Load concentration factor | k | 1 | |
| **Design Torque** | **[Mt]** | **2687100** | **Nmm** |
| **Peak torque** | **[Mtp]** | **6565000** | **Nmm** |
| Gear ratio | i | 1 | |
| Ψ=b/a | Ψ | 0.3 | |
| Young's Modulus (pinion) | E1 | 2.10E+05 | N/mm^2 |
| Young's Modulus (gear) | E2 | 2.10E+05 | N/mm^2 |
| **Eq. Young's Mouduls** | **Eeq.** | **210000** | **N/mm^2** |

| | | | |
|---|---|---|---|
| Design Surface stress | [σc] | 1.55E+03 | N/mm^2 |
| **Minimum centre distance** | **a** | **145.3231646** | **mm** |

| | | | |
|---|---|---|---|
| Pressure angle | ϕn | 20 | deg. |
| Helix angle | β | 25 | deg. |
| Assumed no of teeth in pinion | Z1 | 31 | |
| **Virtual no. of teeth** | **Zv** | **41.64228569** | |
| Form factor based on Zv | yv | 0.467 | |
| Ψm = b/m | Ψm | 10 | |
| Design Bending stress | [σb] | 207 | N/mm^2 |
| **Min normal module** | **mn** | **4.665002221** | **mm** |
| Selected module | mn | 5 | mm |

## Checking

***Performance***

| | | | |
|---|---|---|---|
| **Surface stress** | **σc** | **1214.09** | **N/mm^2** |
| **Bending stress** | **σb** | **183.61** | **N/mm^2** |

***Peak***

| | | | |
|---|---|---|---|
| **Surface stress** | **σc** | **1897.69** | **N/mm^2** |
| **Bending stress** | **σb** | **448.58** | **N/mm^2** |

## Gear Specifications

| | | | |
|---|---|---|---|
| **No of teeth Pinion** | | **31** | |
| **No of teeth Gear** | | **31** | |
| **Addendum** | | **5** | **mm** |
| **Dedendum** | | **6.25** | **mm** |
| **Pinion pitch diameter** | | **171.0236** | **mm** |
| **Gear pitch diameter** | | **171.0236** | **mm** |
| **Pinion base diameter** | | **158.7039** | **mm** |
| **Gear base diameter** | | **158.7039** | **mm** |
| **Standard centre distance** | | **171.0236** | **mm** |
| **Pinion outside diameter** | | **181.0236** | **mm** |
| **Gear outside diameter** | | **181.0236** | **mm** |
| **Pinion root diameter** | | **158.5236** | **mm** |

| | | | |
|---|---|---|---|
| Gear root diameter | | 158.5236 | mm |
| face width | | 60 | mm |

***Forces (Performance)***

| | | | |
|---|---|---|---|
| Tangential Load | Wt | 31423.73748 | N |
| Radial Load | Wr | 12619.66989 | N |
| Axial Load | Wa | 14653.12943 | N |
| Resultant Load | W | 36897.44635 | N |

***Forces (Peak)***

| | | | |
|---|---|---|---|
| Tangential Load | Wt | 76773.04028 | N |
| Radial Load | Wr | 30831.80113 | N |
| Axial Load | Wa | 35799.85662 | N |
| Resultant Load | W | 90146.15582 | N |

**Considering dynamic loading at higher rpms**

| | | | |
|---|---|---|---|
| Form factor for Lewis eq. | Yv | 0.393 | |
| Beam strength of helical gear (acc. To Lewis eq.) | Fs | 69564.69524 | N |
| power | | 280 | HP |
| Load at (max power) | Ft | 10413.4403 | N |
| RPM of pinion (mean assumed) | | 2000 | RPM |
| Mean velocity | | 17.90954715 | m/s |
| Velocity factor | Cv | 3.984924525 | |
| Dynamic load | Fd | 41496.77363 | N |
| | | design is safe | |

**Acc. to Buckingham's dynamic load**

| | | | |
|---|---|---|---|
| Pitch line velocity | Vm | 1074.572829 | m/min |
| error in action | e | 0.25 | mm |
| Dynamic factor | c | 2965 | |
| Buckingham's dynamic load | Fd | 40334.43496 | N |
| | | design is safe | |

**Wear strength of gear tooth by buckingham**

| | | | |
|---|---|---|---|
| Ratio factor | Q | 1 | |
| Load stress factor | k | 15.70079516 | |
| Max. Wear strength of gear tooth | Fw | 827293.9839 | N |
| | | design is safe | |

### 3.3.4 Rating of helical gears

Most prominent reasons of failure for gears include pitting resistance (contact stresses) and bending strength. Rating of the helical gears is done by **ANSI/AGMA 2001-D04**, *Fundamental Rating Factors and Calculation Methods for Involute Spur and Helical Gear Teeth* for both pitting resistance and bending strength.

## Pitting resistance

**Fundamental formula**

The contact stress number formula for gear teeth is:

$$\sigma_H = Z_E \sqrt{F_t K_o K_v K_s \frac{K_H}{d_{w1} b} \frac{Z_R}{Z_I}} \tag{3.38}$$

where

$\sigma_H$ = contact stress number, N/mm$^2$;

$K_o$ = overload factor;

$K_H$ = load distribution factor;

$Z_E$ = elastic coefficient, [N/mm$^2$]$^{0.5}$;

$F_t$ = transmitted tangential load, N;

$Z_R$ = surface condition factor for pitting resistance;

$K_v$ = dynamic factor;

$K_s$ = size factor;

b = net face width of the narrowest member, mm;

$Z_I$ = geometry factor for pitting resistance;

$d_{w1}$ = operating pitch diameter of pinion, mm;

$d_{w1}$ $= \frac{2a}{u+1}$ for external gears

where

a = operating centre distance, mm;

u = gear ratio

**Allowable contact stress number**

The realtion of calculated contact stress number to allowable contact stress number is:

$$\sigma_H \leq \frac{\sigma_{HP}}{S_H} \frac{Z_N}{Y_\theta} \frac{Z_w}{Y_Z} \tag{3.39}$$

where

$\sigma_{HP}$ = allowable contact stress number, N/mm$^2$;

$Z_W$ = hardness ratio factor for pitting resistace;

$Z_N$ = stress cycle factor for pitting resistance;

$Y_\theta$ = temperature factor;

$S_H$ = safety factor for pitting;

$Y_Z$ = reliability factor.

## Bending strength

### Fundamental formula

The fundamental formula for bending stress number in a gear tooth is:

$$\sigma_F = F_t K_o K_v K_s \frac{1}{b\, m_t} \frac{K_H K_B}{Y_J} \tag{3.40}$$

where

$\sigma_F$ = bending stress number, N/mm$^2$;

$K_B$ = rim thickness factor;

$Y_J$ = geometry factor for bending;

$m_t$ = transverse metric module, mm.

$m_t$ $= \frac{m_n}{\cos\beta}$

where

$m_n$ = normal metric module, mm;

$\beta$ = helix angle at standard pitch diameter.

### Allowable bending stress number

The relation of calculated bending stress number to allowable stress number:

$$\sigma_F \le \frac{\sigma_{FP} Y_N}{S_F Y_\theta Y_Z} \tag{3.41}$$

where

$\sigma_{FP}$ = allowable bending stress number, N/mm$^2$;

$Y_\theta$ = temperature factor;

$S_F$ = safety factor for bending;

$Y_N$ = stress cycle factor for bending strength;

$Y_Z$ = reliability factor.

For geometry factors to calculate both values, **AGMA 908-B89, "***Geometry Factors for Determining the Pitting Resistance and Bending Strength of Spur, Helical and Herringbone Gear Teeth"* has been used. Figure 4.2 is an extracted table from AGMA 908-B89 that has been used in this case.

*I* AND *J* FACTORS FOR:[1]

20.0 DEG. PRESSURE ANGLE
25.0 DEG. HELIX ANGLE
0.250 TOOL EDGE RADIUS
EQUAL ADDENDUM ($x_1 = x_2 = 0$)

2.250 WHOLE DEPTH FACTOR
0.024 TOOTH THINNING FOR BACKLASH
LOADED AT TIP

AGMA 908-B89
Page -38

| | | PINION TEETH | | | | | | | | | | | | | | | |
|---|---|---|---|---|---|---|---|---|---|---|---|---|---|---|---|---|---|
| GEAR | | 12 | | 14 | | 17 | | 21 | | 26 | | 35 | | 55 | | 135 | |
| TEETH | | P | G | P | G | P | G | P | G | P | G | P | G | P | G | P | G |
| 12 | I | | | | | | | | | | | | | | | | |
| | J | U | U | | | | | | | | | | | | | | |
| 14 | I | | | 0.123 | | | | | | | | | | | | | |
| | J | U | U | 0.40 | 0.40 | | | | | | | | | | | | |
| 17 | I | | | 0.137 | | 0.126 | | | | | | | | | | | |
| | J | U | U | 0.41 | 0.43 | 0.43 | 0.43 | | | | | | | | | | |
| 21 | I | | | 0.152 | | 0.142 | | 0.130 | | | | | | | | | |
| | J | U | U | 0.41 | 0.45 | 0.44 | 0.45 | 0.46 | 0.46 | | | | | | | | |
| 26 | I | | | 0.167 | | 0.157 | | 0.146 | | 0.134 | | | | | | | |
| | J | U | U | 0.42 | 0.47 | 0.44 | 0.47 | 0.47 | 0.48 | 0.49 | 0.49 | | | | | | |
| 35 | I | | | 0.187 | | 0.178 | | 0.168 | | 0.156 | | 0.138 | | | | | |
| | J | U | U | 0.43 | 0.49 | 0.45 | 0.50 | 0.48 | 0.50 | 0.50 | 0.51 | 0.52 | 0.52 | | | | |
| 55 | I | | | 0.213 | | 0.207 | | 0.199 | | 0.189 | | 0.173 | | 0.144 | | | |
| | J | U | U | 0.44 | 0.52 | 0.46 | 0.52 | 0.49 | 0.53 | 0.51 | 0.54 | 0.53 | 0.55 | 0.56 | 0.56 | | |
| 135 | I | | | 0.248 | | 0.247 | | 0.244 | | 0.239 | | 0.230 | | 0.210 | | 0.151 | |
| | J | U | U | 0.45 | 0.55 | 0.47 | 0.56 | 0.50 | 0.56 | 0.52 | 0.57 | 0.54 | 0.58 | 0.57 | 0.59 | 0.61 | 0.61 |

1 The letter "U" indicates a gear tooth combination which produces an undercut tooth form in one or both components and should be avoided. See Section 7 and Fig 7–1.

Figure 3.15: Geometry factors for pitting resistance and bending strength for helical gears with 25 deg. helix angle and 20 deg. pressure angle

Rating calculations extracted from excel sheet are given below at performance torque:

| Pitting Resistance | | | |
|---|---|---|---|
| Elastic coefficient | ZE | 190 | (N/mm^2)^0.5 |
| **Transmitted tandential load** | **Ft** | **31423.73** | **N** |
| overload factor | Ko | 1 | |
| dynamic factor | Kv | 1.35 | |
| Lead correction factor | KHmc | 0.8 | |
| Pinion proportion factor | KHpf | 0.04 | |

*all constants are taken from ANSI/AGMA 2101-D03

*crowning

| | | | |
|---|---|---|---|
| Pinion proportion modifier | KHpm | 1.1 | |
| Mesh alignment factor | KHma | 0.15 | |
| Mesh alignment Correction factor | KHe | 0.08 | |
| **Load distribution factor** | **KH** | **1.0448** | |
| size factor | Ks | 1 | |
| surface condition factor for pitting resistance | ZR | 1 | |
| **net face width of narrowest member** | **b** | **59.8582521** | **mm** |
| **Normal metric module** | **mn** | **5** | **mm** |
| **Transverse Pressure angle** | **ϕt** | **21.88023267** | **deg.** |
| **geometry factor for pitting resistance** | **ZI** | **0.13576** | |
| gear ratio | mG | 1 | |
| operating center distance | a | 171.0235774 | mm |
| **operating pitch diameter of pinion** | **d** | **171.0235774** | **mm** |
| **Contact stress number** | **σH** | **1131.016154** | **N/mm^2** |
| allowable contact stress number | σHP | 1551 | |
| Stress cycle factor for pitting resistance | ZN | 1 | |
| hardness ratio factor for pitting resistance | ZW | 1 | |
| temperature factor | Yθ | 1 | |
| Reliability factor | YZ | 1 | |
| **Factor of safety** | **σHP** | **1.371333198** | |

| **Bending Strength** | | | |
|---|---|---|---|
| rim thickness factor | KB | 1 | |
| geometry factor for bending strength | YJ | 0.5032 | |
| helix angle at standard pitch diameter | β | 25 | |
| **tranverse metric module** | **mt** | **5.516889595** | **mm** |

| | | | |
|---|---|---|---|
| **bending stress number** | **σF** | **296.3625375** | **N/mm^2** |
| allowable bending stress number | σFP | 400 | **N/mm^2** |
| stress cycle factor for bending strength | YN | 1 | |
| **Factor of safety** | **SF** | **1.349698256** | |

## Factors of safety

Table 3.11: Factors of safety for helical gear

| | **Pitting resistance** | **Bending Strength** |
|---|---|---|
| **Group 1** | 1.94 | 2.72 |
| **Group 2** | 1.45 | 1.50 |
| **Group 3** | 1.45 | 1.50 |

# Chapter 4
## Results

The main aim was to achieve modular design of tandem axle. Various components being used in assembly of tandem axle are designed for entire range of vehicles being manufactured at VECV. Although modular design of hypoid, differential gears and helical gears is individually concluded in their respective sections, following summary sheet can be used for reference to all the components.

Table 4.1: Results (Modular design)

| | | | Hypoid gear | | Helical gear | |
|---|---|---|---|---|---|---|
| Vehicle | | Gear box | Crown gear dia (mm) | Gear face width (mm) | Gear dia | Face width |
| 6x4T 6025 | Onroad | 6s | 350 | 53 | 171.02 | 60 |
| | | zf 9s | 350 | 53 | 171.02 | 60 |
| | | vecv 9s | 350 | 53 | 171.02 | 60 |
| | RMC | 6s | 350 | 53 | 171.02 | 60 |
| | | zf 9s | 350 | 53 | 171.02 | 60 |
| | | vecv 9s | 350 | 53 | 171.02 | 60 |
| | Offroad | 6s | 415 | 60 | 171.02 | 60 |
| | | zf 9s | 415 | 60 | 171.02 | 60 |
| | | vecv 9s | 415 | 60 | 171.02 | 60 |
| 6x4TT | TT | zf 9s | 415 | 60 | 171.02 | 60 |
| | | vecv 9s | 415 | 60 | 171.02 | 60 |
| 8x4T | Tipper | zf 9s | 415 | 60 | 171.02 | 60 |
| | | vecv 9s | 415 | 60 | 171.02 | 60 |
| | RMC | zf 9s | 415 | 60 | 171.02 | 60 |
| | | vecv 9s | 415 | 60 | 171.02 | 60 |
| V1 | Tipper | 9s | 415 | 60 | 171.02 | 60 |
| V2 | Tipper | 9s | 415 | 60 | 171.02 | 60 |
| V3 | TT | 9s | 415 | 60 | 171.02 | 60 |

| | | | | | | |
|---|---|---|---|---|---|---|
| V4 | Tipper | 9s | 440 | 65 | 171.02 | 60 |
| V5 | Tipper | 9s | 440 | 65 | 171.02 | 60 |
| V6 | TT | 9s | 440 | 65 | 171.02 | 60 |

All other specifications are already covered in chapter 3. The results are shown in summary sheet so that we can easily analyse our output design. All of the results are also verified and compared with the help of FEA; however, the organisation's data couldn't be taken out of the system. All the calculation sheets for hypoid gears and helical gears both for design and rating are attached with the file. **(Appendix B)**

# Chapter 5

## Conclusion

The main aim of this project was to develop a modular design of rear tandem axle for heavy duty vehicles. This aim has been accomplished by the modularization of the design of hypoid gear set and helical gear for all the vehicles being manufactured at VECV requiring tandem axle. Calculation sheets for all the gears are made using MS-Excel which includes preliminary design dimensions, ratings of gears for both pitting and bending stresses and final gear specifications. Most prominent causes of gear failure in automotive industry are contact stresses (pitting resistance) and bending strength. All the design parameters, rating formulae and factors are taken from various publications and standards by AGMA. Apart from rating of helical gears using AGMA standards, basic Lewis and Buckingham equations have also been used to check the safety of helical gears.

In case of hypoid gears, complete hypoid geometry design sheet has also been developed which includes a program for an iterative process. Apart from this force analysis is done on both hypoid gear set and helical gears in which tangential, radial and axial forces are calculated.

The modularization approach has helped us to develop common components for a range of vehicles categorized on the basis of application and specifications such as torque and power output.

Future scope of this work may include calculation of reactions at the bearing points using the force analysis done in this study while using CAD data. This will allow us to select the bearings for our assembly..

# References


American Gear Manufacturers Association, (2004). ANSI/AGMA 2101-D04 Fundamental Rating Factors and Calculation Methods for Involute Spur and Helical Gear Teeth. *Alexandria VA: AGMA.*

American Gear Manufacturers Association, (2003). ANSI/AGMA 2005-D03 Design Manual for Bevel Gears.

American Gear Manufacturers Association, (1989). AGMA 908-B89: Geometry Factors for Determining the Pitting Resistance and Bending Strength of Spur, Helical and Herringbone Gear Teeth.

Bagewadi, S.S., Bhavi, I.G. and Kurbet, S.N. (2014). Design and analysis of crown pinion of a differential gear box for reduced number of teeth to improve torque transmitted. *International Journal of Mechanical Engineering and Robotics Research*, *3*(4), p.188.

Baldwin, C. Y. and Clark, K. B. (2000). Design Rules: The Power of Modularity. MIT Press, Cambridge, MA.

Barot, K.K. and Vora, C.P. (2014), January. Design of Rear Axle Gears for Commercial Vehicles. In *International Journal of Engineering Research and Technology* (Vol. 3, No. 1 (January-2014)). ESRSA Publications.

Brnic, J. and Brcic, M. (2015). Comparison of Mechanical Properties and Resistance to Creep of 20MnCr5 Steel and X10CrAlSi25 Steel. *Procedia Engineering*, *100*, pp.84-89.

Brnic, J., Turkalj, G., Lanc, D., Canadija, M., Brcic, M. and Vukelic, G. (2014). Comparison of material properties: Steel 20MnCr5 and similar steels. *Journal of Constructional Steel Research*, 95, pp.81-89.

Brown, M.D. (2009). Design and analysis of a spiral bevel gear (Doctoral dissertation, Rensselaer Polytechnic Institute).

Coleman, W. (1967). Paper 13: Bevel and Hypoid Gear Surface Durability: Pitting and Scuffing. In *Proceedings of the Institution of Mechanical Engineers, Conference*

*Proceedings* (Vol. 182, No. 1, pp. 191-204). Sage UK: London, England: SAGE Publications.

Dana corporation (2005). *Inter-axle differential with improved differential gear mounting arrangement*. US6884196 B1.

Dana corporation (2007). *Service Manual(AXSM0042).* Dana ® Spicer ® Tandem Drive Axles

Dana Spicer Tandem Drive Axles. (2007). Service Manual, AXSM0042.

Davis, J.R. ed. (2005). *Gear materials, properties, and manufacture*. ASM International.

Duffy, J.E. (2000). *Modern automotive technology*. Goodheart-Willcox Company.

Gamba, A. and Fusari, N. (2009). Valuing modularity as a real option. *Management science*, *55*(11), pp.1877-1896.

Gawande, S.H., Khandagale, S.V., Jadhav, V.T., Patil, V.D. and Thorat, D.J. (2013). Design, Manufacturing & Analysis of Differential Crown Gear and Pinion for MFWD Axle. *Department of Mechanical Engineering, MES College of Engineering, Pune*.

Gligorijević, R., Jevtić, J. And Borak, D. (2008) Material Selection In Gear Design.

Griffith, B. (1990). Hypoid Gear Design for Automotive Axles. *Gear Design, Manufacturing and Inspection Manual,* Society of Automotive Engineers, Warrendale, PA, pp, 83-103.

Hölttä-Otto, K.(2005). *Modular product platform design*. Helsinki University of Technology.

Hwang, S.C., Lee, J.H., Lee, D.H., Han, S.H. and Lee, K.H. (2013). Contact stress analysis for a pair of mating gears. *Mathematical and Computer Modelling*, *57*(1), pp.40-49.

Jyothirmai, S., Ramesh, R., Swarnalatha, T. and Renuka, D. (2014). A finite element approach to bending, contact and fatigue stress distribution in helical gear systems. *Procedia Materials Science*, *6,* pp.907-918.

Kakavas, I., Olver, A.V. and Dini, D. (2016). Hypoid gear vehicle axle efficiency. *Tribology International*, *101*, pp.314-323.

Kashkoush, M. and ElMaraghy, H. (2016). Optimum Overall Product Modularity. *Procedia CIRP*, *44*, pp.55-60.

Langlois, R.N., (2002). Modularity in technology and organization. *Journal of economic behavior & organization*, *49*(1), pp.19-37.

Lim, T. and Cheng, Y. (1999). A Theoretical Study of the Effect of Pinion Offset on the Dynamics of Hypoid Geared Rotor System. *Journal of Mechanical Design*, 121(4), p.594.

Malek, T.A. and Solanki, A.B. (2015). A Review: Design, Modeling and Stress Analysis of high speed helical gear according to Bending strength and Contact strength using AGMA and ANSYS. *International Journal of trends and technology*, *22*, pp.526-530.

PSG, (2008). Design data. *Kalaikathir Achchagam publishers, Coimbatore India*

Radzevich, S.P. and Dudley, D.W. (1994). *Handbook of practical gear design*. CRC press.

Salvador, F., Forza, C. and Rungtusanatham, M. (2002). Modularity, product variety, production volume, and component sourcing: theorizing beyond generic prescriptions. *Journal of operations management*, *20*(5), pp.549-575.

Sekercioglu, T. and Kovan, V. (2007). Pitting failure of truck spiral bevel gear. *Engineering Failure Analysis*, *14*(4), pp.614-619.

Shigley, J.E. (2011). *Shigley's mechanical engineering design*. Tata McGraw-Hill Education.

Stokes, A. (1992). *Manual gearbox design*. Butterworth-Heinemann.

Thomas, J. (1984). *Design and Manufacture of Spiral Bevel and Hypoid Gears for Heavy-Duty Drive Axles, 1984* (No. 841085). SAE Technical Paper.

Venkatesh, B., Kamala, V. and Prasad, A.M.K. (2010). Design, Modelling and Manufacturing of Helical Gear. *International journal of applied engineering research, Dindigul*, *1*, pp.103-114.

Venkatesh, J. and Murthy, M.P. (2014). Design and Structural Analysis of High Speed Helical Gear Using Ansys. *International Journal of Engineering Research and Applications*, *2*(3), pp.215-232.

# Appendix A

**Detail formulae to calculate hypoid geometry** (Design of bevel gear, ANSI-AGMA 2005-D03)

| Item | Pinion | Both pinion and gear | Gear |
|---|---|---|---|
| Pitch diameter | | | $D = \frac{N}{P_d}$ |
| (metric) | | | $(D = N m_{et})$ |
| Gear ratio | | $m_G = \frac{N}{n}$ | |
| Desired pinion spiral angle | $\psi_{oP} = \psi_P$ | | |
| Shaft angle departure from 90° | | $\Delta\Sigma = \Sigma - 90$ | |
| Approximate gear pitch angle | | | $\tan\Gamma_i = \frac{m_G(\cos\Delta\Sigma)}{1.2(1 - m_G \sin\Delta\Sigma)}$ |
| Gear mean pitch radius | | | $R = \frac{D - F\sin\Gamma_i}{2}$ |
| Approximate pinion offset angle in pitch plane | $\sin\varepsilon'_{2i} = \frac{E\sin\Gamma_i}{R}$ | | |
| Approximate hypoid dimension factor | | $K_1 = \tan\psi_{oP}\sin\varepsilon'_{2i} + \cos\varepsilon'_{2i}$ | |
| Approximate pinion mean radius | $R_{2P} = \frac{RK_1}{m_G}$ | | |
| | | **Start of iteration** | |
| | | First trial | |
| Gear offset angle in axial plane | | | $\tan\eta = \frac{E}{R(\tan\Gamma_i\cos\Delta\Sigma - \sin\Delta\Sigma) + R_{2P}}$ |
| | | Second trial | |
| Intermediate pinion offset angle in axial plane | $\sin\varepsilon_2 = \frac{E - R_{2P}\sin\eta}{R}$ | | |
| Intermediate pinion pitch angle | $\tan\gamma_2 = \frac{\sin\eta}{\tan\varepsilon_2\cos\Delta\Sigma} + \tan\Delta\Sigma\cos\eta$ | | |
| Intermediate pinion offset angle in pitch plane | $\sin\varepsilon'_2 = \frac{\sin\varepsilon_2\cos\Delta\Sigma}{\cos\gamma_2}$ | | |
| Intermediate pinion mean spiral angle | $\tan\psi_{2P} = \frac{K_1 - \cos\varepsilon'_2}{\sin\varepsilon'_2}$ | | |
| Increment in hypoid dimension factor | | $\Delta K = \sin\varepsilon'_2(\tan\psi_{oP} - \tan\psi_{2P})$ | |
| Ratio of pinion mean radius increment to gear mean pitch radius | | $\frac{\Delta R_P}{R} = \frac{\Delta K}{m_G}$ | |
| Pinion offset angle in axial plane | $\sin\varepsilon_1 = \sin\varepsilon_2 - \frac{\Delta R_P}{R}\sin\eta$ | | |
| Pinion pitch angle | $\tan\gamma = \frac{\sin\eta}{\tan\varepsilon_1\cos\Delta\Sigma} + \tan\Delta\Sigma\cos\eta$ | | |
| Pinion offset angle in pitch plane | $\sin\varepsilon'_1 = \frac{\sin\varepsilon_1\cos\Delta\Sigma}{\cos\gamma}$ | | |

*(continued)*

| Item | | Pinion | Both pinion and gear | Gear |
|---|---|---|---|---|
| Spiral angle | | $\tan\psi_P = \dfrac{K_1 + \Delta K - \cos\varepsilon'_1}{\sin\varepsilon'_1}$ | | $\psi_G = \psi_P - \varepsilon'_1$ |
| Gear pitch angle | | | | $\tan\Gamma = \dfrac{\sin\varepsilon_1}{\tan\eta\cos\Delta\Sigma} + \cos\varepsilon_1\tan\Delta\Sigma$ |
| Mean cone distance | | | | $A_{mG} = \dfrac{R}{\sin\Gamma}$ |
| Pinion mean radius increment | | $\Delta R_P = \left(\dfrac{\Delta R_P}{R}\right)R$ | | |
| Mean cone distance | | $A_{mP} = \dfrac{R_{2P} + \Delta R_P}{\sin\gamma}$ | | |
| Mean pinion radius | | $R_P = A_{mP}\sin\gamma$ | | |
| Limit pressure angle | | | $(-\tan\phi_o) = \dfrac{\tan\gamma\tan\Gamma}{\cos\varepsilon'_1}\left(\dfrac{A_{mP}\sin\psi_P - A_{mG}\sin\psi_G}{A_{mP}\tan\gamma + A_{mG}\tan\Gamma}\right)$ | |
| Mean tooth curvature | Face Hobbing | | $N_c = \dfrac{N}{\sin\Gamma}$<br>$\sin\nu = \dfrac{A_{mG}N_s}{r_c N_c}\cos\psi_G$<br>$\lambda = 90° - \psi_G + \nu$<br>$S_1 = \sqrt{A_{mG}^2 + r_c^2 - 2A_{mG}r_c\cos\lambda}$<br>$\cos\eta_1 = \dfrac{A_{mG}\cos\psi_G}{S_1 N_c}(N_c + N_s)$<br>$\rho = A_{mG}\cos\psi_G\left[\tan\psi_G + \dfrac{\tan\eta_1}{1 + \tan\nu(\tan\psi_G + \tan\eta_1)}\right]$ | |
| | Face Milling | $\rho = r_c$ | | |
| Iteration factor | Method 1<br>Hypoid radius of curvature (Face milling or face hobbing) | Calculate the following | $r_{c1} = \dfrac{\sec\phi_o(\tan\psi_P - \tan\psi_G)}{(-\tan\phi_o)\left(\dfrac{\tan\psi_P}{A_{mP}\tan\gamma} + \dfrac{\tan\psi_G}{A_{mG}\tan\Gamma}\right) + \dfrac{1}{A_{mP}\cos\psi_P} - \dfrac{1}{A_{mG}\cos\psi_G}}$<br>$\Delta = \left\lvert\dfrac{\rho}{r_{c1}} - 1\right\rvert$ | |
| | Method 2 (Face hobbing only) | Calculate the following | $\Delta = \dfrac{r_c\cos(\psi_G - \nu)}{A_{mG}\sin\Gamma - r_c\sin\Gamma\sin(\psi_G - \nu)} - \dfrac{n\cos\psi_G\sin\varepsilon'_1}{N\cos\psi_P\sin\gamma - n\cos\psi_G\cos\varepsilon'_1}$ | |
| Testing for convergence | | | Change $\eta$ until $\lvert\Delta\rvert \le 0.001$ | |
| | | | **End of iteration** | |
| Pressure angle concave | | $\phi_1 = \phi + \phi_o$ | | $\phi_2 = \phi - \phi_o$ |
| Pressure angle convex | | $\phi_2 = \phi - \phi_o$ | | $\phi_1 = \phi + \phi_o$ |
| Crossing point to mean point along gear axis | | $Z_G = A_{mP}\tan\gamma\sin\Gamma - \dfrac{E\tan\Delta\Sigma}{\tan\varepsilon_1}$ | | |
| Gear pitch apex beyond crossing point | | | | $Z = \dfrac{R}{\tan\Gamma} - Z_G$ |
| Outer cone distance | | | | $A_{oG} = \dfrac{0.5D}{\sin\Gamma}$ |

*(continued)*

| Item | Pinion | Both pinion and gear | Gear |
|---|---|---|---|
| Gear face width from calculation point to outside | | | $\Delta F_o = A_{oG} - A_{mG}$ |
| Equivalent 90° ratio | | $m_{90} = \sqrt{\left(\dfrac{\sin\Sigma - \cos\Sigma}{\tan(\Sigma - \Gamma)}\right)\dfrac{\cos\gamma\cos\eta}{\cos\Gamma}}$ | |
| Depth factor | | $k_1$ (See table 4) | |
| Mean addendum factor | | $c_1$ (See table 5) | |
| Mean working depth | | $h = \dfrac{2k_1 R\cos\psi_G}{N}$ | |
| Mean addendum | $a_P = h - a_G$ | | $a_G = c_1 h$ |
| Clearance factor | | $k_2$ (See 7.5) | |
| Mean dedendum | $b_P = b_G + a_G - a_P$ | | $b_G = h(1 + k_2 - c_1)$ |
| Clearance | | $c = k_2 h$ | |
| Mean whole depth | | $h_m = a_G + b_G$ | |
| Sum of dedendum angles | | $\Sigma\delta$ (See table 6) | |
| Dedendum angle | | | $\delta_G$ (See table 7) |
| Addendum angle | | | $\alpha_G = \Sigma\delta - \delta_G$ |
| Outer addendum | | | $a_{oG} = a_G + \Delta F_o \sin\alpha_G$ |
| Outer dedendum | | | $b_{oG} = b_G + \Delta F_o \sin\delta_G$ |
| Gear whole depth | | | $h_{tG} = a_{oG} + b_{oG}$ |
| Outer working depth | | $h_k = h_{tG} - c$ | |
| Root angle | | | $\Gamma_R = \Gamma - \delta_G$ |
| Face angle | | | $\Gamma_o = \Gamma + \alpha_G$ |
| Gear outside diameter | | | $D_o = 2a_{oG}\cos\Gamma + D$ |
| Gear crown to crossing point | | | $X_o = Z_G + \Delta F_o\cos\Gamma - a_{oG}\sin\Gamma$ |
| Root apex beyond crossing point | | | $Z_R = Z + \dfrac{A_{mG}\sin\delta_G - b_G}{\sin\Gamma_R}$ |
| Face apex beyond crossing point | | | $Z_o = Z - \dfrac{A_{mG}\sin\alpha_G - a_G}{\sin\Gamma_o}$ |
| Auxiliary angle for calculating pinion offset angle in root plane | $\tan\zeta_R = \dfrac{E\tan\Delta\Sigma\cos\Gamma_R}{A_{mG}\cos\delta_G - Z\cos\Gamma_R}$ | | |
| Auxiliary angle for calculating pinion offset angle in face plane | $\tan\zeta_o = \dfrac{E\tan\Delta\Sigma\cos\Gamma_o}{A_{mG}\cos\alpha_G - Z\cos\Gamma_o}$ | | |
| Pinion offset angle plus auxiliary angle in root plane | $\sin(\varepsilon_R + \zeta_R) = \dfrac{E\cos\zeta_R\sin\Gamma_R}{A_{mG}\cos\delta_G - Z\cos\Gamma_R}$ | | |
| Pinion offset angle plus auxiliary angle in face plane | $\sin(\varepsilon_o + \zeta_o) = \dfrac{E\cos\zeta_o\sin\Gamma_o}{A_{mG}\cos\alpha_G - Z\cos\Gamma_o}$ | | |
| Face angle | $\sin\gamma_o = \sin\Delta\Sigma\sin\Gamma_R + \cos\Delta\Sigma\cos\Gamma_R\cos\varepsilon_R$ | | |
| Root angle | $\sin\gamma_R = \sin\Delta\Sigma\sin\Gamma_o + \cos\Delta\Sigma\cos\Gamma_o\cos\varepsilon_o$ | | |
| Face apex beyond crossing point | $G_o = \dfrac{E\sin\varepsilon_R\cos\Gamma_R - Z_R\sin\Gamma_R - c}{\sin\gamma_o}$ | | |

*(continued)*

| Item | Pinion | Both pinion and gear | Gear |
|---|---|---|---|
| Root apex beyond crossing point | $G_R = \dfrac{E \sin \varepsilon_o \cos \Gamma_o - Z_o \sin \Gamma_o - c}{\sin \gamma_R}$ | | |
| Addendum angle | $\alpha_P = \gamma_o - \gamma$ | | |
| Dedendum angle | $\delta_P = \gamma - \gamma_R$ | | |
| Angle between projection of pinion axis into pitch plane and pitch element | $\tan \lambda' = \dfrac{\sin \varepsilon'_1 \cos \Gamma}{m_G \cos \gamma + \cos \Gamma \cos \varepsilon'_1}$ | | |
| Gear face width from calculating point to inside | | | $\Delta F_i = F_G - \Delta F_o$ |
| Pinion face width increment | $\Delta F_{oP} = h \sin \varepsilon_R \left(1 - \dfrac{1}{m_G}\right)$ | | |
| Pinion face width from a calculating point to outside | $F_{oP} = \dfrac{\Delta F_o \cos \lambda'}{\cos(\varepsilon'_1 - \lambda')}$ | | |
| Pinion face width from calculating point to inside | $F_{iP} = \dfrac{\Delta F_i \cos \lambda'}{\cos(\varepsilon'_1 - \lambda')}$ | | |
| Increment along pinion axis from calculating point to outside | $\Delta B_o = \dfrac{F_{oP} \cos \gamma_o}{\cos \alpha_P} + \Delta F_{oP} - (b_G - c) \sin \gamma$ | | |
| Increment along pinion axis from calculating point to inside | $\Delta B_i = \dfrac{F_{iP} \cos \gamma_o}{\cos \alpha_P} + \Delta F_{oP} + (b_G - c) \sin \gamma$ | | |
| Crown to crossing point | $x_o = \dfrac{E}{\tan \varepsilon_1 \cos \Delta\Sigma} - R_P \tan \gamma + \Delta B_o$ | | |
| Front crown to crossing point | $x_i = \dfrac{E}{\tan \varepsilon_1 \cos \Delta\Sigma} - R_P \tan \gamma - \Delta B_i$ | | |
| Whole depth, pinion | $h_{tP} = \dfrac{(x_o + G_o) \sin(\gamma_o - \gamma_R)}{\cos \gamma_o} - \sin \gamma_R (G_R - G_o)$ | | |
| Outside diameter | $d_o = 2 \tan \gamma_o (x_o + G_o)$ | | |
| Face width | $F_P = \dfrac{x_o - x_i}{\cos \gamma_o}$ | | |
| Mean circular pitch | | $p_m = \dfrac{\pi}{P_d}\left(\dfrac{A_{mG}}{A_{oG}}\right)$ | |
| Mean diametral pitch | | $P_{dm} = P_d \dfrac{A_{oG}}{A_{mG}}$ | |
| Thickness factor | | $k_3$ (See figure 21) | |
| Mean pitch diameter | $d_m = 2A_{mP} \sin \gamma$ | | $D_m = 2A_{mG} \sin \Gamma$ |
| Pitch diameter | $d = 2(A_{mP} + 0.5F_P) \sin \gamma$ | | |
| Mean normal circular tooth thickness, theoretical without backlash | $t_n = p_m \cos \psi - T_n$ | | $T_n = 0.5 p_m \cos \psi_G - (a_P - a_G) \tan \phi - \dfrac{k_3 \cos \psi_G}{P_{dm}}$ |
| Outer normal backlash allowance | | $B$ (See table 8) | |
| Outer gear spiral angle face milling | | | $\sin \psi_{oG} = \dfrac{2A_{mG} r_c \sin \psi_G - A_{mG}^2 + A_{oG}^2}{2A_{oG} r_c}$ |

*(continued)*

| Item | Pinion | Both pinion and gear | Gear |
|---|---|---|---|
| Outer gear spiral angle face hobbing | | | $Q = \frac{S_1}{1 + \frac{N_s}{N_c}}$ <br> $\cos\eta_o = \frac{A_{oG}^2 + S_1^2 - r_c^2}{2A_{oG}\, S_1}$ <br> $\tan\psi_{oG} = \frac{A_{oG} - Q\cos\eta_o}{Q\sin\eta_o}$ |
| Mean normal chordal tooth thickness | $t_{nc} = t_n - \left(\frac{t_n^3}{6d_m^2}\right) - 0.5B\left\{\frac{\frac{A_{mG}}{A_{oG}}}{\cos\phi\frac{\cos\psi_G}{\cos\psi_{oG}}}\right\}$ | | $T_{nc} = T_n - \left(\frac{T_n^3}{6D_m^2}\right) - 0.5B\left\{\frac{\frac{A_{mG}}{A_{oG}}}{\cos\phi\frac{\cos\psi_G}{\cos\psi_{oG}}}\right\}$ |
| Mean chordal addendum | $a_{cP} = a_P + \frac{0.25t_n^2\cos\gamma}{d_m}$ | | $a_{cG} = a_G + \frac{0.25T_n^2\cos\Gamma}{D_m}$ |

# Appendix B

To view Excel calculation sheets for hypoid and helical gears, visit:

https://drive.google.com/drive/folders/0B9NZkFun9Ua6UGV0WDVaT3FPWWs?usp=sharing